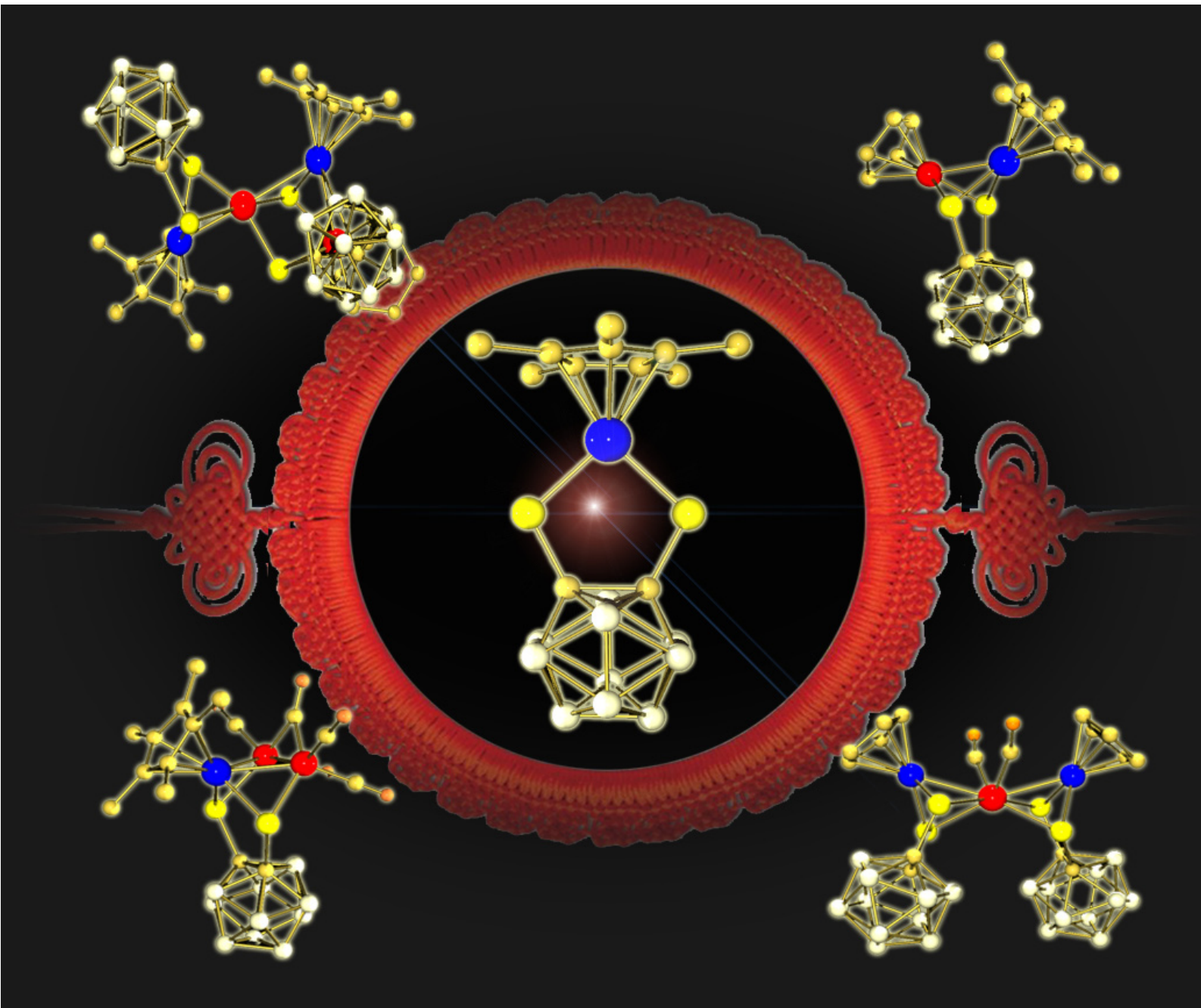


Chem Soc Rev

Chemical Society Reviews

www.rsc.org/chemsocrev

Volume 36 | Number 10 | October 2007 | Pages 1533 - 1696



ISSN 0306-0012

TUTORIAL REVIEW

Shuang Liu, Ying-Feng Han and Guo-Xin Jin

Formation of direct metal–metal bonds from 16-electron “pseudo-aromatic” half-sandwich complexes $Cp^*M[E_2C_2(B_{10}H_{10})]$

TUTORIAL REVIEW

Tsuyoshi Satoh

Recent advances in the chemistry of magnesium carbenoids



0306-0012(2007)36:10;1-Y

RSC Publishing

Formation of direct metal–metal bonds from 16-electron “pseudo-aromatic” half-sandwich complexes $\text{Cp}^*\text{M}[\text{E}_2\text{C}_2(\text{B}_{10}\text{H}_{10})]^\dagger$

Shuang Liu, Ying-Feng Han and Guo-Xin Jin*

Received 23rd March 2007

First published as an Advance Article on the web 8th May 2007

DOI: 10.1039/b701869j

Continuous study on preparation of multimetallic clusters is stimulated by their rich coordination chemistry and promising applications in a variety of interesting fields. Although numerous efforts have been devoted to this field, the rational design of *homo*- and *hetero*-multimetallic compounds with direct metal–metal bonding supported by 1,2-dicarba-*closo*-dodecarborane-1,2-dichalcogenolates will still be an important step forward. This *tutorial review* focuses on the synthetic approach *via* redox reactions between the pseudo-aromatic half-sandwich organometallic carborane precursors and low-valent transition metal reagents. The tailoring of reaction conditions and the structural information from the resulting products are discussed extensively.

1 Introduction

The synthesis of structurally defined multinuclear complexes has been receiving tremendous attention and emphasis during recent decades,^{1,2} in particular complexes containing direct metal–metal bonds. The greatest stimulus for the development of this research field is the cooperative interaction of two or more coordination centers,³ which offers attractive perspectives in stoichiometric and catalytic transformations.⁴ Furthermore, multimetallic clusters have even found medical applications.⁵ Traditionally, the synthetic approaches are designed mainly based on photochemistry,⁶ direct synthesis from metal oxides or halides,⁷ and sometimes even on serendipitous discoveries.⁸ Whatever the procedure, the use of bridging ligands to bring two metal centers within bonding

(or interaction) distance has played a decisive role in the systematic investigation of such systems. Among the bridging ligands commonly utilized,^{9–11} dithiolene ligands have attracted particular attention as ancillary groups in the rational design of multi-metallic complexes, due to their coordinative unsaturation in the planar MS_2C_2 subunits.^{12,13}

1,2-Dicarba-*closo*-dodecarborane-1,2-dichalcogenolates (*ortho*-carborane dichalcogenolates), the three-dimensional super-aromatic analogue of the benzene counterpart,¹⁴ are of particular interest as sterically demanding, chemically robust chelating dichalcogenolato ligands. They are easily prepared by the insertion of elemental chalcogen into the Li–C bonds of dilithium carborane after deprotonation by *n*-butyllithium; they exhibit potential to function as promising ligands to facilitate the formation of direct metal–metal bonding. Not only can these ligands serve as promising candidates for construction of desired clusters like other dithiolenes, but additional superior features can also be anticipated: (1) these bulky ligands are expected to increase the stability of the multinuclear complexes due to the highly conjugated system;

Shanghai Key Laboratory of Molecular Catalysis and Innovative Materials, Department of Chemistry, Fudan University, Shanghai, China 200433. E-mail: gxjin@fudan.edu.cn.

† Cp^* = $\eta^5\text{-C}_5\text{Me}_5$, $\eta^5\text{-C}_5\text{H}_5$ or $\eta^5\text{-1,3-Bu}^t\text{C}_5\text{H}_3$ or $\eta^6\text{-4-isopropyl-toluene}$.



Shuang Liu

and was engaged in the study of carbene catalysts for olefin polymerization supported by the Chun-Tsung Fellowship.

Shuang Liu was born in 1983 in Inner Mongolia, P. R. China. She received her BS degree in the year of 2004 in Chemistry Department at Fudan University, and was promoted to a Master Program afterward. She is now studying under the guidance of Prof. Guo-Xin Jin. Her research interest is currently focused on the design of multinuclear clusters with dichalcogenolato carboranyl ligands. She was awarded the Excellent Graduate of Shanghai in 2004,



Ying-Feng Han

Ying-Feng Han was born in 1980 in Shandong, P. R. China. He received his MS degree in the year of 2006 in Chemistry Department at South China Normal University. Since 2006 he has been a PhD candidate at Fudan University in the group of Prof. Jin. His current research interests are in molecular architecture via self-assembly using half-sandwich transition metal complexes as subunits and metal cluster complexes with carborane dichalcogenolato ligands.

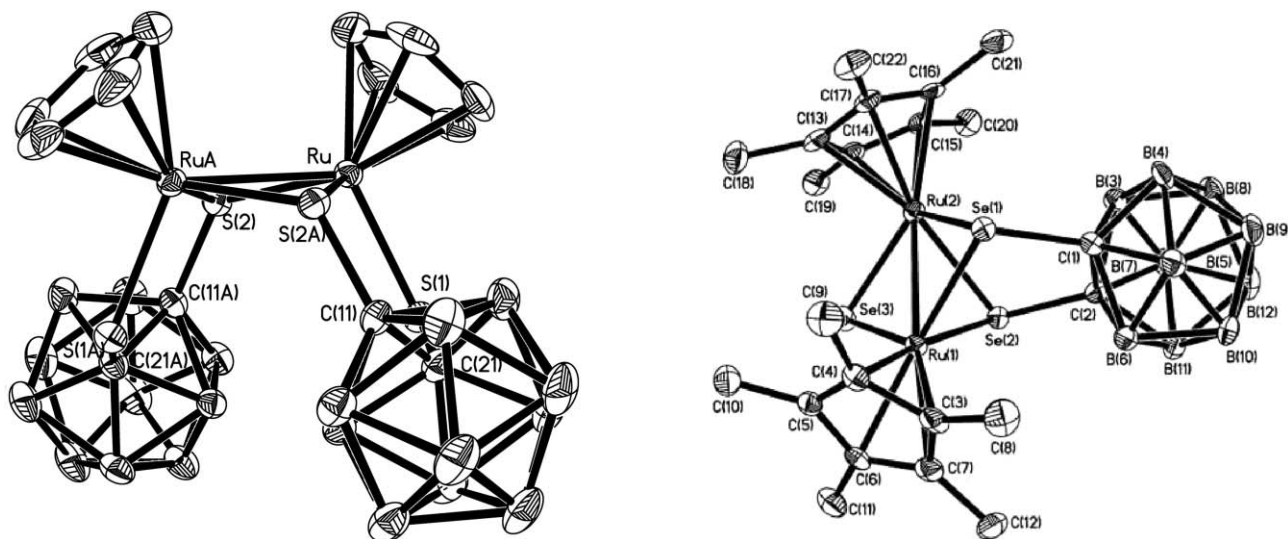


Fig. 1 Molecular structures of **1a** and **2b**.

from this aspect, coordination reactions at the pseudo-aromatic MS_2C_2 metallacycles can proceed under relatively mild conditions in most cases; (2) the icosahedral symmetry of the carboranyl unit, together with the cyclopentadienyl ligands, can dramatically increase the solubility of the resulting clusters, and hence improve the common problem of crystallization; (3) the inherent characteristics of the carborane cluster may affect the chemical and physical properties of the resulted products, and pave the way for practical applications.

The past decade has seen a rapid development of systematic studies on the versatility of 1,2-dicarba-*closo*-dodecarborane-1,2-dichalcogenolates in metal–metal bonding formation, since the first attempt made in 1997, which effectively bridges the two best developed areas of polyhedral boranes and metal clusters in inorganic cluster chemistry. A recent review concerning the chemistry of mononuclear organometallic

complexes with 1,2-dichalcogenolato-*o*-carborane ligands served as the basis for the present topic.¹⁵ Although metalladithiolene complexes employed in transformations toward multinuclear entities has been already well-documented,¹³ up to now there is no review article focusing on the specific research field of carboranyl dichalcogenolates. Therefore, we summarize in this *tutorial review* the recent investigations on the syntheses of homo- and hetero-multinuclear clusters with ancillary 1,2-dichalcogenolato carborane ligands as a general and facile approach, and the crystallographic evidence of direct metal–metal bond formation. This collection of works centers exclusively on the *ortho*-carborane dichalcogenolates, although a few examples of metalacarborane complexes are included due to the fact that it is indispensable to discuss the reactivity under different conditions. Since most of the studies are based on half-sandwich transition metal dichalcogenolates as precursors, the following discussion will be classified according to different reagents involved.

2 Serendipitous discoveries of bimetallic complexes

During the direct syntheses of a number of mononuclear half-sandwich carboranyl complexes of Co, Rh, Ir and Ru, as described in the previous review,¹⁵ dinuclear Cp and Cp* ($Cp = \eta^5-C_5H_5$; $Cp^* = \eta^5-C_5Me_5$) half-sandwich complexes containing bridging $[E_2C_2(B_{10}H_{10})]^{2-}$ ($E = S, \mathbf{a}$; Se, \mathbf{b})[‡] ligands are observed serendipitously. For example, attempts to combine the $[E_2C_2(B_{10}H_{10})]^{2-}$ building block with a 17e fragment, $[CpRu(PPh_3)_2]$ or $[Cp^*RuCl_2]$, did not give a mononuclear product but a symmetrical bimetallic complex $(CpRu)_2-[S_2C_2(B_{10}H_{10})]_2$ (**1a**) or $(Cp^*Ru)_2(\mu-Se)[Se_2C_2(B_{10}H_{10})]$ (**2b**), and the Ru–Ru distances of 2.7781 and 2.7177 Å correspond to a single bond (Fig. 1).¹⁶

This trend of forming bimetallic complexes with direct metal–metal bond also occurred in the reaction of dimerized rhodium



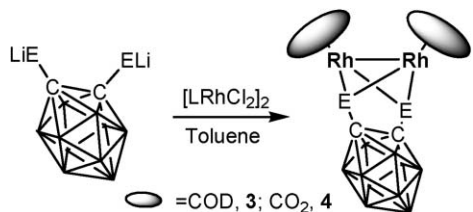
Guo-Xin Jin

Professor Guo-Xin Jin received his PhD from Nanjing University in 1987, and after post-doctoral work at University of Bayreuth, Germany, he joined Changchun Institute of Applied Chemistry, Chinese Academy of Sciences in 1996 as a professor. In 2001 he moved to Shanghai and held the Chair Professor (CheungKong Scholarship) of Inorganic Chemistry at Fudan University. He is now a Regional Associate Editor of

Dalton Transactions and serves as a member of Editorial Boards for *Organometallics* and *Journal of Organometallic Chemistry*. His research interests are in organometallic Chemistry, particularly of metal cluster complexes with carborane dichalcogenolato ligands, half-sandwich metal chalcogenide complexes and catalysts for olefin polymerization.

[‡] Unless otherwise specified, E stands for a chalcogen element, with suffix **a** for sulfur and **b** for selenium in this article.

complex $[\text{Rh}(\text{COD})(\mu\text{-Cl})_2]_2$ (COD = 1,5-cyclooctadiene, C_8H_{12}) or $[\text{Rh}(\text{CO})_2(\mu\text{-Cl})]_2$ with $\text{Li}_2\text{E}_2\text{C}_2\text{B}_{10}\text{H}_{10}$ (Scheme 1), which affords the dirhodium complexes $(\text{LRh})_2[\text{E}_2\text{C}_2\text{B}_{10}\text{H}_{10}]$ (L = COD, **3**; 2CO , **4**)¹⁷ at room temperature.

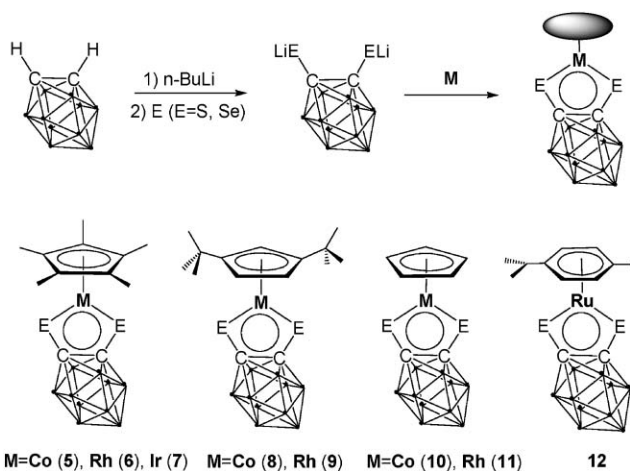


Scheme 1 Synthetic route for dirhodium complexes (**3**, **4**).

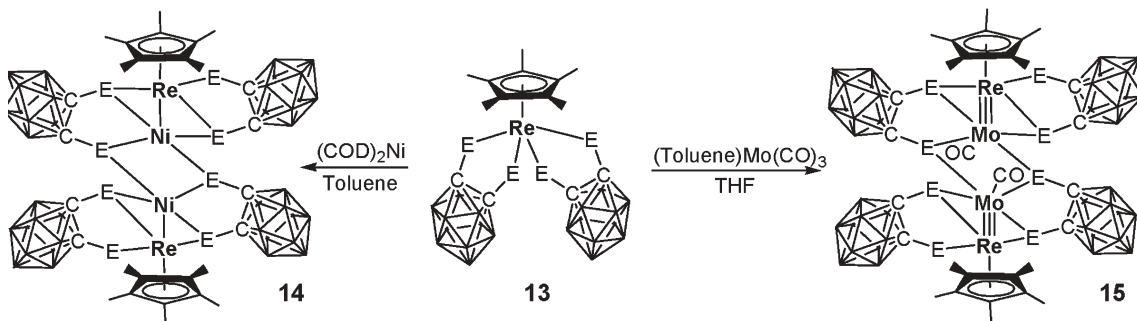
This type of seeming accidental results revealed the strong tendency of the central metals to form a saturated 18e configuration. To study the potential of this series of transition metal complexes, investigations have been extended to the rational design and methodologic versatility for the systematic preparation of such multi-metallic frameworks, in which direct metal–metal bonds are formed between the metal centers.

3 Approaches toward rational design of transition metal clusters

Among the mononuclear 16-electron Cp^* half-sandwich carbonyl complexes synthesized and characterized during the



Scheme 2 Synthesis of the 16e half-sandwich carborane complexes.



Scheme 3 First attempts to prepare multinuclear complexes with direct M–M bonds.

last decade, the most thoroughly studied species are a series of Group 8 (Ru and Os)¹⁸ and Group 9 (Co,¹⁹ Rh²⁰ and Ir²¹) complexes (Scheme 2), partially due the ease of preparation and the relative stability of the pseudo-aromatic system.

In view of the nucleophilic behavior of chalcogen ligands and easy formation of μ -chalcogen bridges in hetero-bimetallic complexes, it is not surprising that the neutral half-sandwich rhenium dichalcogenolate carborane complexes of $\text{Cp}^*\text{Re}[\text{E}_2\text{C}_2(\text{B}_{10}\text{H}_{10})]_2$ (E = S, Se; **13**) act as organometallic bidentate ligands through their chalcogen atoms. Thus, the complexes $\text{Cp}^*\text{Re}[\text{E}_2\text{C}_2(\text{B}_{10}\text{H}_{10})]_2$ (**13**) react with $(\text{COD})_2\text{Ni}$ to give $[\text{Cp}^*\text{Re}(\text{S}_2\text{C}_2\text{B}_{10}\text{H}_{10})_2\text{Ni}]_2$ (**14**) (Fig. 2) and with the toluene-stabilized tricarbonyl molybdenum fragment $(\text{C}_7\text{H}_8)\text{Mo}(\text{CO})_3$ to give the hetero-tetranuclear complexes $[\text{Cp}^*\text{Re}(\text{E}_2\text{C}_2\text{B}_{10}\text{H}_{10})_2\text{Mo}(\text{CO})_2]_2$ (**15**) (Scheme 3).¹⁵ The Re–Ni distances (2.4744 Å) and the capping angles (Re–S–Ni 66.52°) in the other two planes indicate the strong direct interaction between Re and Ni atoms; while the short bond distances between Re and Mo (2.5868 Å, and 2.6205 Å for the diselenolate counterpart) also lie in the range for triple bonds, so that each of Mo and Re centers in the complexes is formally an 18-electron system. This is the very beginning of the vast possibilities for direct metal–metal bonding.

3.1 Carbonyl reagents

Extensive exploration suggests that direct homo- and hetero-metal bonding between ruthenium or group 9 metals (Co, Rh, Ir) and transition metals namely Mo, W, Fe and Co can be accomplished by reacting 16-electron 1,2-dicarba-*closo*-dodecarborane-1,2-dichalcogenolato precursors (**5–12**) with carbonyl transition metal reagents.

Mo(CO)₃(py)₃. The combination of $\text{Mo}(\text{CO})_3(\text{py})_3$ (py = pyridine, NC_5H_5 ; **16**) and BF_3 has been used as an effective way to generate a reactive $[\text{Mo}(\text{CO})_3]$ fragment in previous study.²² In this way, complexes **5–12** (**a**, **b**) can react with $\text{Mo}(\text{CO})_3(\text{py})_3$ (**16**) in the presence of more than three equivalents of $\text{BF}_3 \cdot \text{Et}_2\text{O}$ to give a series of bi- or tri-metallic mixed-metal complexes. Representative structures are presented in Scheme 4.

In the reaction between $\text{Cp}^*\text{Co}[\text{E}_2\text{C}_2(\text{B}_{10}\text{H}_{10})]$ (**5**) and $\text{Mo}(\text{CO})_3(\text{py})_3$ (**16**), the sole product in high yields is the purple binuclear $\text{Cp}^*\text{Co}[\text{E}_2\text{C}_2(\text{B}_{10}\text{H}_{10})]\text{Mo}(\text{CO})_2[\text{E}_2\text{C}_2(\text{B}_{10}\text{H}_{10})]$ (**17**).²³ The binuclear complex **17** contains two *o*-carborane thiolato ligands: one serves as the bridging ligand

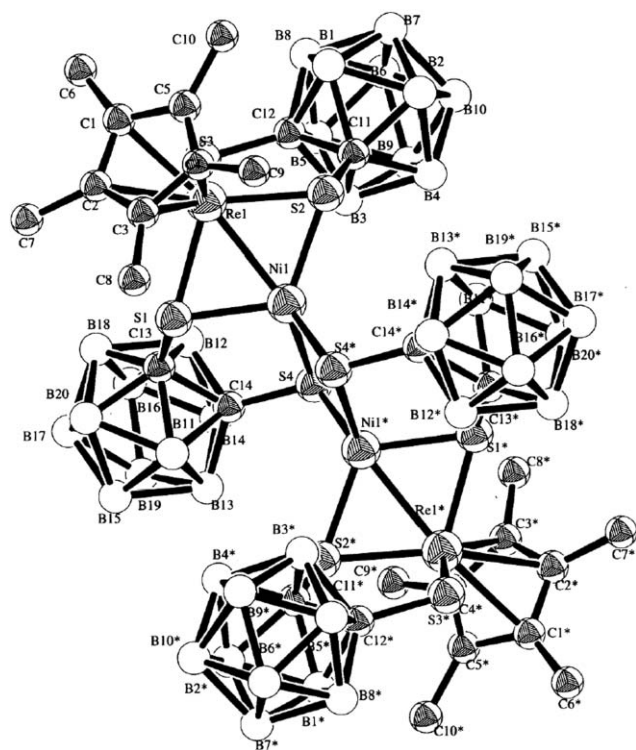
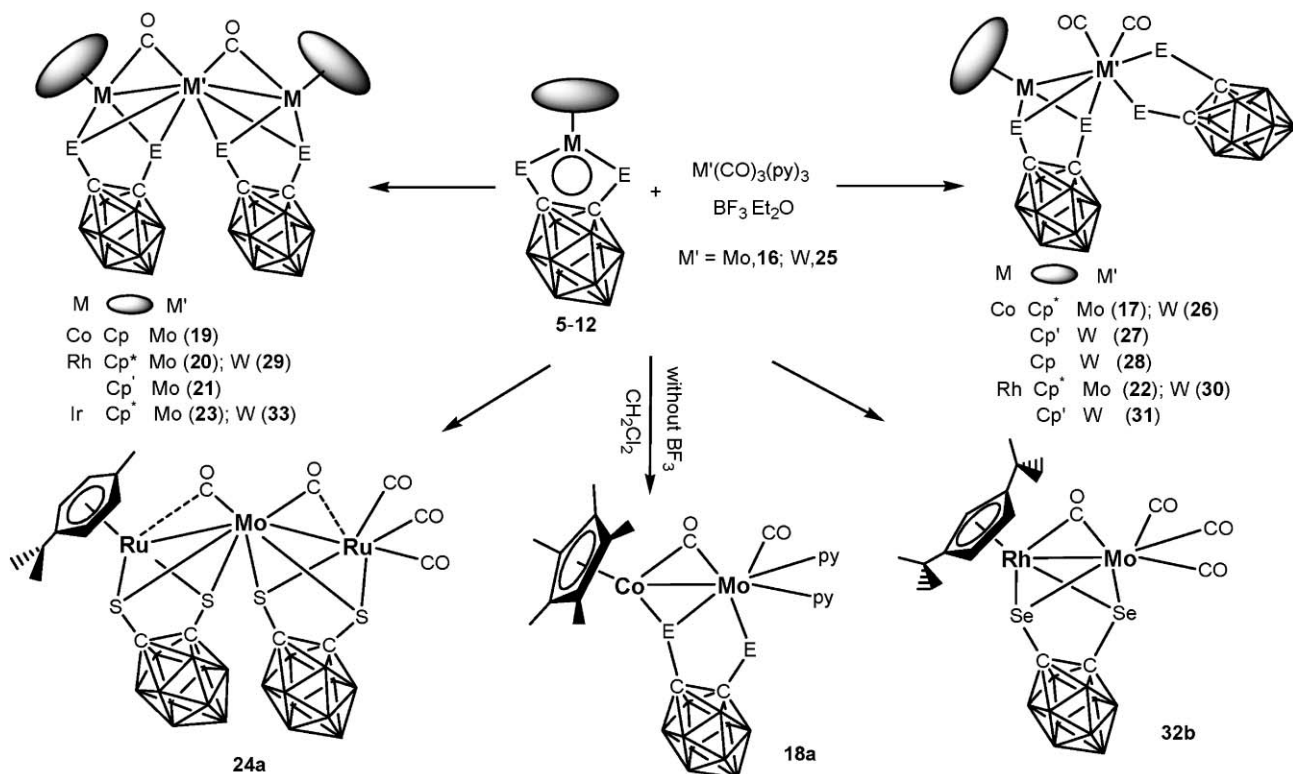


Fig. 2 Molecular structure of 14a.

and the other is attached only to the $[\text{Mo}(\text{CO})_2]$ fragment. The molybdenum atom shows seven-coordination geometry, having two terminal carbonyl ligands, the pseudo-aromatic system of the cobaladithiolen heterocycle in 17 is folded by 138° along

the $\text{S}\cdots\text{S}$ vector, due to the coordination of the S atoms to Mo; while the five-membered metallacycle MoS_2C_2 is nearly planar. If performed in the absence of $\text{BF}_3\cdot\text{Et}_2\text{O}$ using dichloromethane as solvent, red binuclear complexes $\text{Cp}^*\text{Co}(\mu_2\text{-CO})[\text{E}_2\text{C}_2(\text{B}_{10}\text{H}_{10})]\text{Mo}(\text{CO})(\text{py})_2$ (18) can be formed in moderate yields (Fig. 3). The Mo, further coordinated by two pyridine groups and one carbonyl group, has a total of 16 valence electrons. The distance between cobalt and molybdenum is 2.501 \AA in 18a, clearly indicating a single metal–metal bond nature. Unlike the bridging carbonyl group in 17a, there is a stronger interaction between cobalt and the bridging CO group ($\text{Co}(1)\text{-C}(3) 2.171 \text{ \AA}$); this may account for a shorter Co–Mo bond (2.501 \AA) than the average single bond. $\{\text{CpCo}[\text{E}_2\text{C}_2(\text{B}_{10}\text{H}_{10})]\}_2\text{Mo}(\text{CO})_2$ (19), a trimetallic product is formed by the reaction of $\text{CpCo}[\text{E}_2\text{C}_2(\text{B}_{10}\text{H}_{10})]$ (10) with $\text{Mo}(\text{CO})_3(\text{py})_3$ (16)/ $\text{BF}_3\cdot\text{Et}_2\text{O}$, which comprises two dichalcogenolato metal centers bridged by a molybdenum dicarbonyl unit (Fig. 3).

Meanwhile, when reacted with rhodium species $\text{Cp}^*\text{Rh}[\text{E}_2\text{C}_2(\text{B}_{10}\text{H}_{10})]$ (6) and $\text{Cp}'\text{Rh}[\text{E}_2\text{C}_2(\text{B}_{10}\text{H}_{10})]$ ($\text{Cp}' = \eta^5\text{-1,3-Bu}^t\text{C}_5\text{H}_3$, 9), the main products are trinuclear Rh–Mo–Rh species, namely $\{\text{Cp}^*\text{Rh}[\text{E}_2\text{C}_2(\text{B}_{10}\text{H}_{10})]\}_2\text{Mo}(\text{CO})_2$ (20)²⁴ and $\{\text{Cp}'\text{Rh}[\text{E}_2\text{C}_2(\text{B}_{10}\text{H}_{10})]\}_2\text{Mo}(\text{CO})_2$ (21).²⁵ They all exhibit similar configurations as the cobalt counterpart 19. Bimetallic byproduct $\text{Cp}^*\text{Rh}[\text{S}_2\text{C}_2(\text{B}_{10}\text{H}_{10})]\text{Mo}(\text{CO})_2[\text{S}_2\text{C}_2(\text{B}_{10}\text{H}_{10})]$ (22a) is observed only in the case of 6a (Fig. 4). The Mo–Rh interaction is a single bond if taking into account the bond length (2.745 \AA), so this arrangement does not satisfy the 18-electron rule in Mo center, and thus the complex is coordinatively unsaturated. The reaction of the iridium 16-electron precursor $\text{Cp}^*\text{Ir}[\text{Se}_2\text{C}_2(\text{B}_{10}\text{H}_{10})]$ (7b) can only give



Scheme 4 Reactions with $\text{Mo}(\text{CO})_3(\text{py})_3$ (16) and $\text{W}(\text{CO})_3(\text{py})_3$ (25).

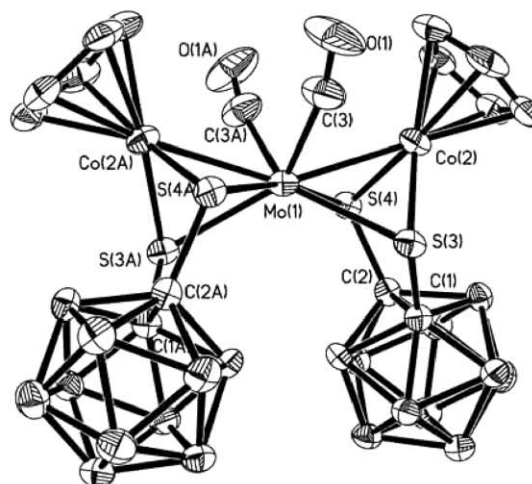
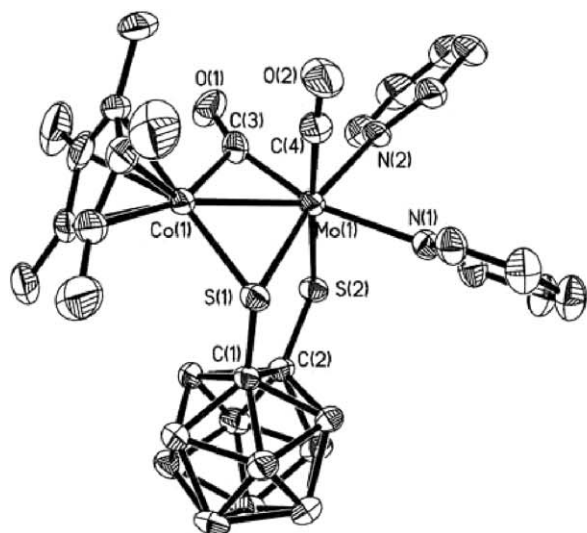


Fig. 3 Molecular structures of 18a and 19a.

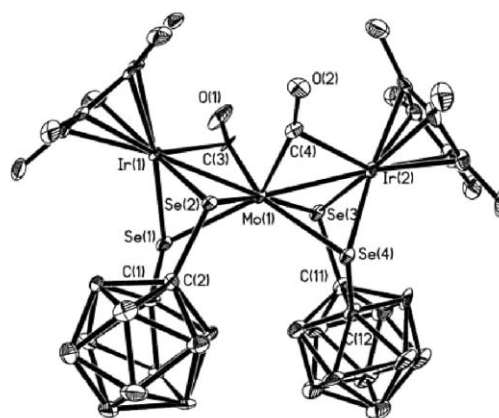
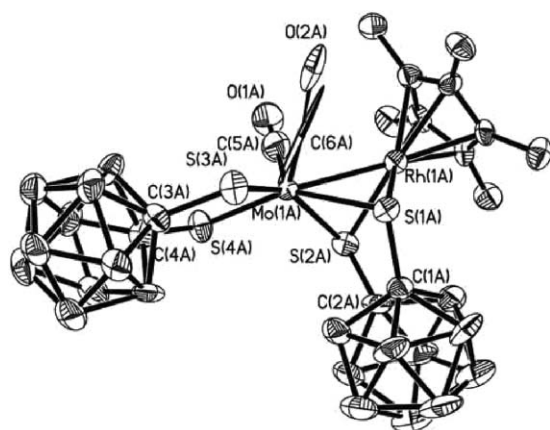


Fig. 4 Molecular structures of 22a and 23b.

trinuclear product $\{\text{Cp}^*\text{Ir}[\text{S}_2\text{C}_2(\text{B}_{10}\text{H}_{10})]\}_2\text{Mo}(\text{CO})_2$ (**23b**) as depicted in Fig. 4.²⁶

Interestingly, in the case of ruthenium $[(p\text{-cymene})\text{Ru}\{\text{S}_2\text{C}_2(\text{B}_{10}\text{H}_{10})\}]$ ($p\text{-cymene} = \eta^6\text{-4-isopropyltoluene}$, **12a**), substitution of the shielding $p\text{-cymene}$ group by three carbonyls is observed besides the formation of the trinuclear cluster $\{(p\text{-cymene})\text{Ru}[\text{S}_2\text{C}_2(\text{B}_{10}\text{H}_{10})]\}_2\text{Mo}(\text{CO})_2$ (**24a**) (Fig. 5).²⁷

Therefore, the combination of $\text{Mo}(\text{CO})_3(\text{py})_3/\text{BF}_3$ with mononuclear 16e half-sandwich carborane complexes can successfully lead to syntheses of multinuclear clusters containing Group 9 metals and ruthenium. Direct M–Mo bonding lies in the range of single bond interactions, namely 2.626 Å (Co–Mo), 2.755–2.826 Å (Rh–Mo), 2.782–2.819 Å (Ir–Mo) and 2.789–2.819 Å (Ru–Mo), each supported by a symmetrically bridging *ortho*-carborane-1,2-dichalcogenolato ligand. The former planar pseudo-aromatic systems of the MS_2C_2 are usually folded in the electronically saturated products, with the dihedral angles at the E⋯E vector ranging from 135 to 140°.

$\text{W}(\text{CO})_3(\text{py})_3$. The reactions of complexes **5–11** with $\text{W}(\text{CO})_3(\text{py})_3$ (**25**) and BF_3 in diethyl ether are comparable

to the molybdenum analogue (Scheme 4). The formation of the neutral and diamagnetic mixed-metal complexes involves redox processes during which the group 9 metal centers (Co, Rh and Ir) are partially reduced by the low-valence tungsten fragment $[\text{W}(\text{CO})_3]$. The main products, trimetallic clusters, can be obtained in higher yields only upon heating/refluxing or when longer reaction times is applied, due to the lower reactivity of W centers compared to Mo.

The reaction between the 16-electron half-sandwich cobalt complexes **5**, **8** and **10** with $\text{W}(\text{CO})_3(\text{py})_3$ (**25**) lead only to the formation of hetero-bimetallic products, namely $\text{Cp}^*\text{Co}[\text{E}_2\text{C}_2(\text{B}_{10}\text{H}_{10})]\text{W}(\text{CO})_2[\text{E}_2\text{C}_2(\text{B}_{10}\text{H}_{10})]$ (**26**),²³ $\text{Cp}^*\text{Co}[\text{E}_2\text{C}_2(\text{B}_{10}\text{H}_{10})]\text{W}(\text{CO})_2[\text{E}_2\text{C}_2(\text{B}_{10}\text{H}_{10})]$ (**27**)²⁸ and $\text{CpCo}[\text{E}_2\text{C}_2(\text{B}_{10}\text{H}_{10})]\text{W}(\text{CO})_2[\text{E}_2\text{C}_2(\text{B}_{10}\text{H}_{10})]$ (**28**).²³ In these complexes, tungsten atom is seven-coordinated with capped trigonal prism coordination geometry, and the non-bridging carboranyl ligand has a distorted envelop conformation (Fig. 6). The Co–W bond length varies from 2.653 to 2.705 Å.

The purple/red trinuclear and binuclear complexes containing direct Rh–W bonding are obtained from half-sandwich rhodium carborane dichalcogenolato complexes **6** and **9**, $\{\text{Cp}^*\text{Rh}[\text{E}_2\text{C}_2(\text{B}_{10}\text{H}_{10})]\}_2\text{W}(\text{CO})_2$ (**29**), $\text{Cp}^*\text{Rh}[\text{S}_2\text{C}_2(\text{B}_{10}\text{H}_{10})]$

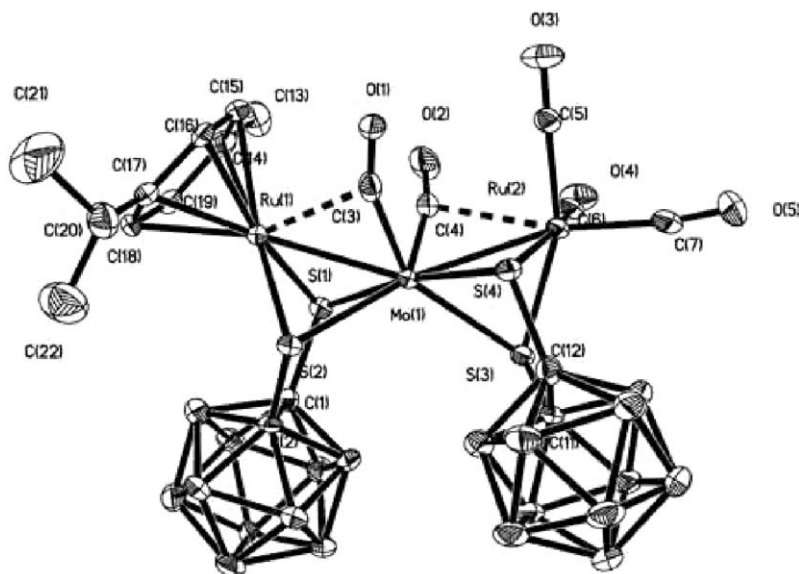


Fig. 5 Molecular structure of 24a.

$W(CO)_2[S_2C_2(B_{10}H_{10})]$ (**30a**),²⁹ $Cp^*Rh[S_2C_2(B_{10}H_{10})W(CO)_2-S_2C_2(B_{10}H_{10})]$ (**31a**) and $\{Cp^*Rh[Se_2C_2(B_{10}H_{10})]\}(\mu-CO)-[W(CO)_3]$ (**32b**),²⁴ respectively. The Rh–W bonds lie in the same range, around 2.75 Å, in both the bimetallic and trimetallic compounds.

At room temperature, the desired product $\{Cp^*Ir[E_2C_2(B_{10}H_{10})]\}_2W(CO)_2$ (**33**) can be isolated only in quite low quantities in the case of iridium, whereas high-yield formation is achieved by refluxing the mixture in toluene for 12 h.^{30,31} Dark red prismatic crystals are obtained after chromatography on silica gel and recrystallization from toluene–hexane (Fig. 7). The Ir–W bond is about 2.79 Å according to single-crystal X-ray analysis.

Fe(CO)₅. The interaction of unsaturated hydrocarbons with carbonyl complexes such as $Fe(CO)_5$ (**34**) has been recognized as one of the most important reactions in the field of organometallic chemistry, which makes $Fe(CO)_5$ (**34**) a

promising reagent for reactions with a pseudo-aromatic ring in half-sandwich carboranyl complexes. To investigate the possible extension of the synthetic approach for M–Fe clusters, attempts were made to react the model complexes, $Cp''Co[E_2C_2(B_{10}H_{10})]$ ($Cp'' = Cp^*$ (**5**), Cp (**10**)),³² $Cp''Rh[E_2C_2(B_{10}H_{10})]$ ($Cp'' = Cp^*$ (**6**), Cp' (**9**))³² and $Cp^*Ir[E_2C_2(B_{10}H_{10})]$ (**7**),³³ with **34** in the presence of two equivalents of Me_3NO (Scheme 5).

Complexes $Cp^*Co[E_2C_2(B_{10}H_{10})]Fe(CO)_3$ (**35**) were obtained from the reactions of the 16-electron complexes **5** with $Fe(CO)_5$ (**34**) at room temperature overnight, and the yield was about 26%. While the similar reaction between **10** and **35** could not proceed at room temperature; when the temperature was raised to about 50 °C, the toluene solution gradually turned brown from yellow–green. After chromatography, the neutral air-sensitive, brown hetero-binuclear complexes $CpCo[E_2C_2(B_{10}H_{10})]Fe(CO)_3$ (**36**) could be obtained in about 25% yields. Complexes **36** are more

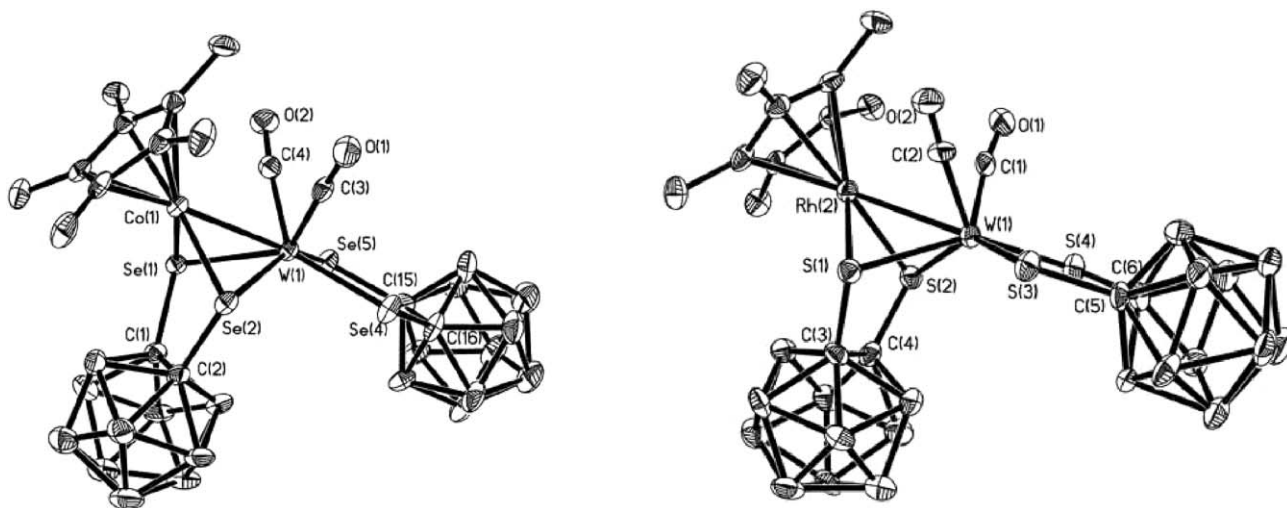


Fig. 6 Molecular structures of 26b and 30a.

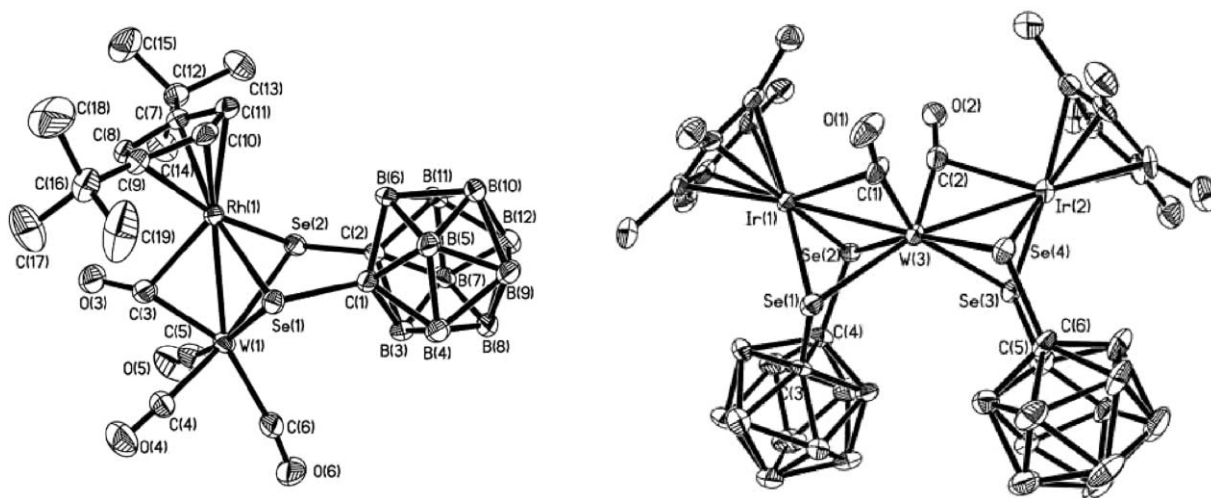
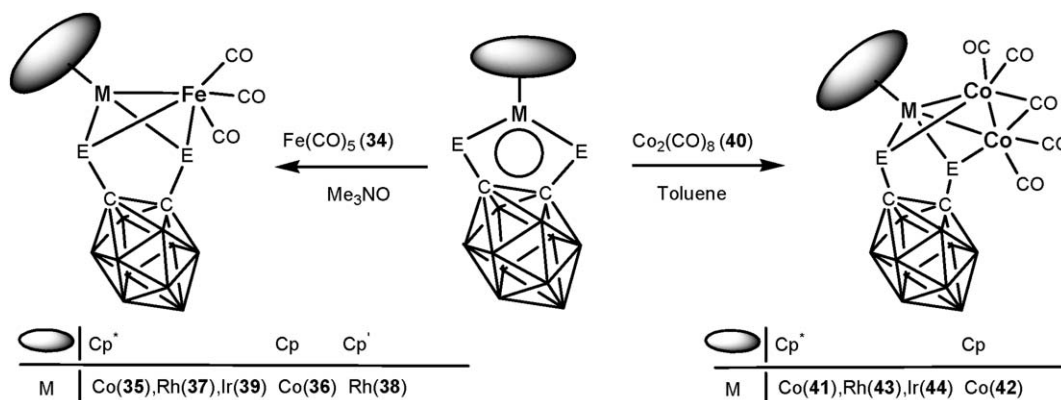


Fig. 7 Molecular structures of 32b and 33b.



Scheme 5 Reactions with $\text{Fe}(\text{CO})_5$ (34) and $\text{Co}_2(\text{CO})_8$ (40).

air- and moisture-sensitive than their analogs 35. The products of rhodium and iridium species, $\text{Cp}^*\text{Rh}[\text{E}_2\text{C}_2(\text{B}_{10}\text{H}_{10})]\text{Fe}(\text{CO})_3$ ($\text{Cp}^* = \text{Cp}^*$ (37), Cp' (38))³² and $\text{Cp}^*\text{Ir}[\text{E}_2\text{C}_2(\text{B}_{10}\text{H}_{10})]\text{Fe}(\text{CO})_3$ (39)³³ can be obtained in higher yields (around 50%) at ambient conditions, and they are relatively more stable compared with the corresponding cobalt analogues.

All these mixed-metal products exhibit typical vibration absorptions of terminal CO ligands in the solid state, typically at 2038 vs and 1963 vs cm^{-1} in IR spectra. Through X-ray crystal structure analysis, complexes 35–39 show similar structures as depicted selectively in Fig. 8 and Fig. 9. Direct M–Fe interactions are observed and the $[\text{Cp}^*\text{M}]$ and $[\text{Fe}(\text{CO})_3]$ units are bridged by two μ_3 -chalcogen atoms from the bridging carboranyl ligands. Both the group 9 metal and iron are six-coordinated with a distorted trigonal-bipyramidal geometry, if the cyclopentadienyl group and its derivatives are viewed as three coordination ligands. The bond lengths are found to be in the range expected for a single bond: 2.398–2.423 Å (Co–Fe), 2.513–2.550 Å (Rh–Fe) and 2.576 Å (Ir–Fe), respectively. The C–O bond lengths in the terminal carbonyls are not significantly different from one another and are similar to the corresponding distances of those in $\text{Fe}_2(\text{CO})_9$.³⁴

$\text{Co}_2(\text{CO})_8$. It has been found that precursors 5–7 and 10 can react readily with $\text{Co}_2(\text{CO})_8$ (40) in a 1 : 1 molar ratio at room temperature, and the reactions proceed quickly, judging from the immediate color change. The crystallized products, $\text{Cp}^*\text{Co}[\text{E}_2\text{C}_2(\text{B}_{10}\text{H}_{10})]\{\text{Co}_2(\text{CO})_5\}$ ($\text{Cp}^* = \text{Cp}^*$, 41; Cp , 42),²³

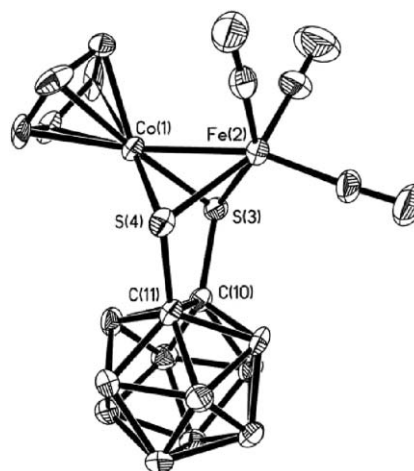


Fig. 8 Molecular structure of 36a.

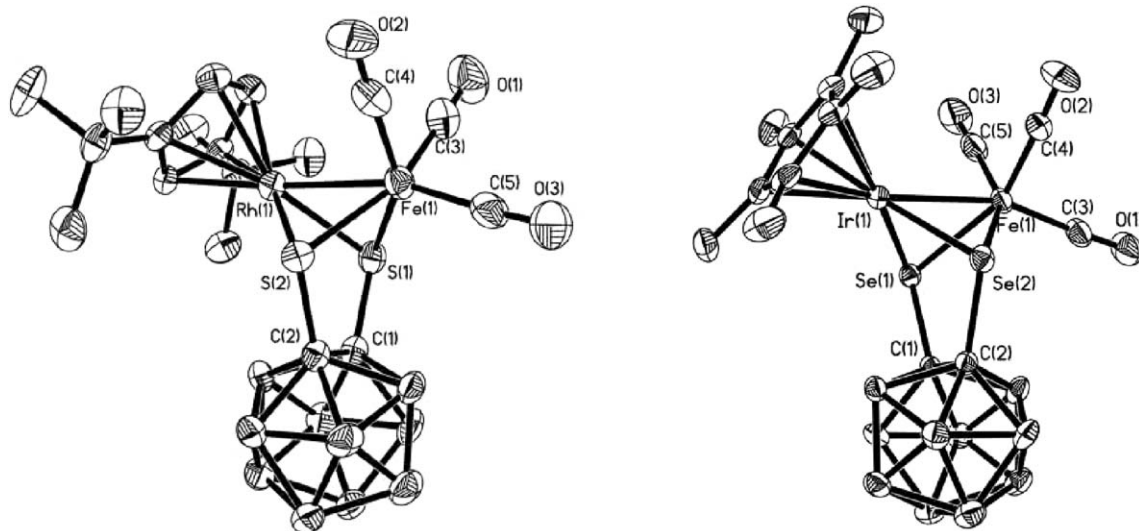


Fig. 9 Molecular structures of **38a** and **39b**.

$\{\text{Cp}^*\text{Rh}[\text{E}_2\text{C}_2(\text{B}_{10}\text{H}_{10})]\}\{\text{Co}_2(\text{CO})_5\}$ (**43**)²⁹ and $\{\text{Cp}^*\text{Ir}[\text{E}_2\text{C}_2(\text{B}_{10}\text{H}_{10})]\}\{\text{Co}_2(\text{CO})_5\}$ (**44**),³³ can be isolated through chromatography on silica gel in yields of more than 70%. It is noteworthy that, in the presence of the decarbonylation reagent Me_3NO , the products can be obtained in higher yields, and for iridium species this reagent can also prevent the concomitant formation of the byproducts $\text{Cp}^*\text{Ir}(\text{CO})[\text{E}_2\text{C}_2(\text{B}_{10}\text{H}_{10})]$ (**45**). All the products are neutral, diamagnetic, and air-sensitive in solution. In the IR spectra, two bands at around 1800v cm^{-1} indicate the existence of CO bridges besides typical absorptions of the terminal carbonyls. Apparently, there are two types of $\nu(\text{CO})$ frequencies for the $\text{Co}_2(\text{CO})_5$ moieties. However, the ^{13}C NMR spectra in CDCl_3 solution show only one peak for all the CO groups.

Instead of the approximately linear arrangement of metal centers in the previously discussed clusters, the three metal cores in complexes **41–44** form a closed triangular backbone,

with two newly formed M–Co (M = Co, Rh and Ir) bonds and one Co–Co bond retained from the $\text{Co}_2(\text{CO})_5$.

In tricobalt complex **41a**, the distance between the three Co atoms are 2.588, 2.550 and 2.444 Å respectively, which clearly indicates bonding interactions between them (Fig. 10). The bond length of the $\text{Co}(2)\text{--Co}(3)$ from the $\text{Co}_2(\text{CO})_5$ moiety is slightly shorter than that of $\text{Co}(1)\text{--Co}(2)$ and $\text{Co}(1)\text{--Co}(3)$. This may be partly caused by the different bridging ligands; the Co–Co inherited from the reagent is bridged by an additional $\mu_2\text{-CO}$ ligand besides the $\mu_3\text{-S}$ ligands. Complex **43** has a closed $[\text{RhCo}_2]$ triangular core, in which the three M–M edges are bridged together by $\mu_3\text{-chalcogenolato}$ carboranyl ligands. The Rh–Co distances (2.6057, 2.6399 Å) are very short, and the Co–Co distance is comparable to those in **41a**. Similarly, complexes **44** also contain three metal atoms, with a triangular core similar to their analogues. Direct interactions between Ir and Co are shown by bond lengths between 2.597 and 2.646 Å (Fig. 11).

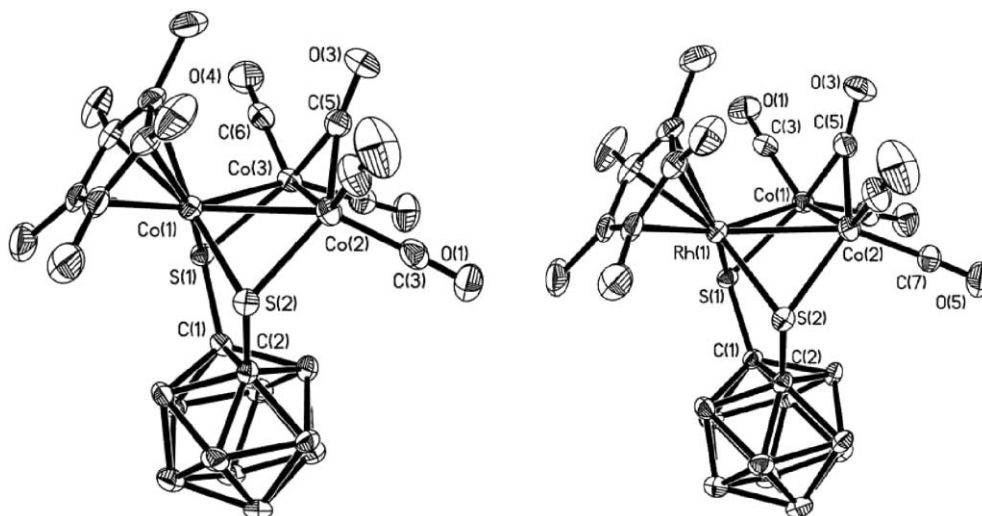


Fig. 10 Molecular structures of **41a** and **43a**.

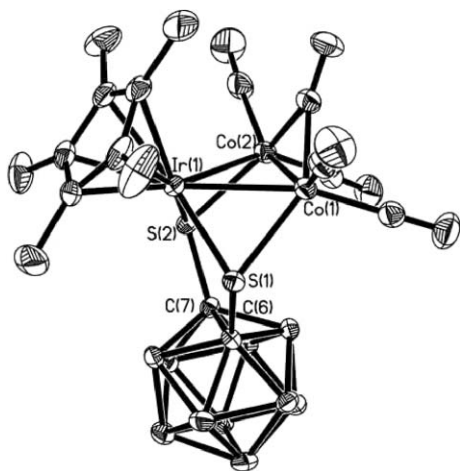


Fig. 11 Molecular structure of 44a.

3.2 Reagents functionalized with COD ligands

$\text{Ni}(\text{COD})_2$. Previously, the low-valent $\text{Ni}(\text{COD})_2$ (**46**) has been applied in the reaction with one and a half equivalents of $\text{Li}_2\text{E}_2\text{C}_2\text{B}_{10}\text{H}_{10}$ ($\text{E} = \text{S}, \text{Se}$) in THF solution in air at room temperature to give the homo-binuclear complexes $[\text{Li}(\text{THF})_4]_2[\text{Ni}_2(\text{E}_2\text{C}_2\text{B}_{10}\text{H}_{10})_3]$ (**47**), in which the two nickel atoms are bridged by a dithiolato carborane to give a binuclear structure with a metal–metal interaction of 2.656 Å (**47a**) (Fig. 12).³⁵ Further investigations have been carried out to explore the reaction of highly reactive reagent toward hetero-multinuclear clusters.

The related reaction between **10** and $\text{Ni}(\text{COD})_2$ (**46**) in toluene leads to the air- and moisture-sensitive, brown hetero-trinuclear complexes $\{\text{CpCo}[\text{E}_2\text{C}_2(\text{B}_{10}\text{H}_{10})]\}_2\text{Ni}$ (**48**) in about 30% yields (Scheme 6),²³ whereas **5** essentially does not react with **46**, even when high temperature and prolonging of the reaction time were introduced. As illustrated in Fig. 13, the molecule of **48a** contains a C_2 axis, the four sulfur atoms from the *o*-carborane dithiolate surrounding the central nickel atom in a distorted tetrahedral arrangement, and the two S–Ni–S planes are twisted by 68.6° due to the repulsion of the bulky

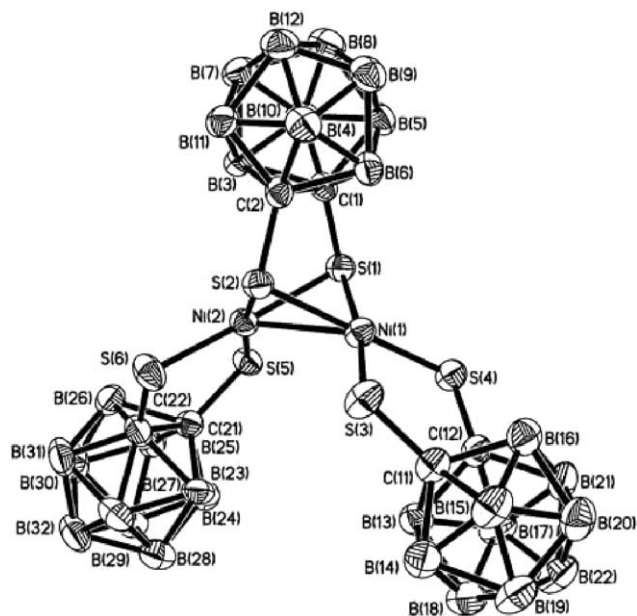
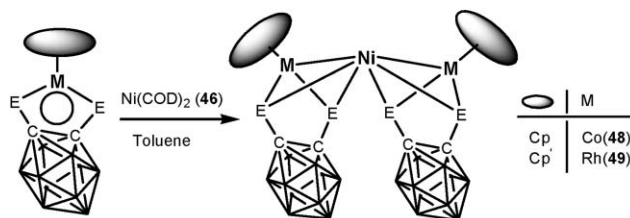


Fig. 12 Molecular structure of 47a.



Scheme 6 Reactions with $\text{Ni}(\text{COD})_2$ (**46**).

cyclopentadienyl ligands. The bond distance between nickel and cobalt is 2.364 Å, indicating a single metal–metal bond.³⁶

Unlike the cobalt counterpart **10**, rhodium precursor **9** can react with $\text{Ni}(\text{COD})_2$ in toluene readily, producing violet hetero-trinuclear complexes $\{\text{Cp}'\text{Rh}[\text{E}_2\text{C}_2(\text{B}_{10}\text{H}_{10})]\}_2\text{Ni}$ (**45**) in about 50% yields.²⁵ The molecular structure of **49a** is depicted in Fig. 13, and is comparable to that of **48a**. The two S–Ni–S

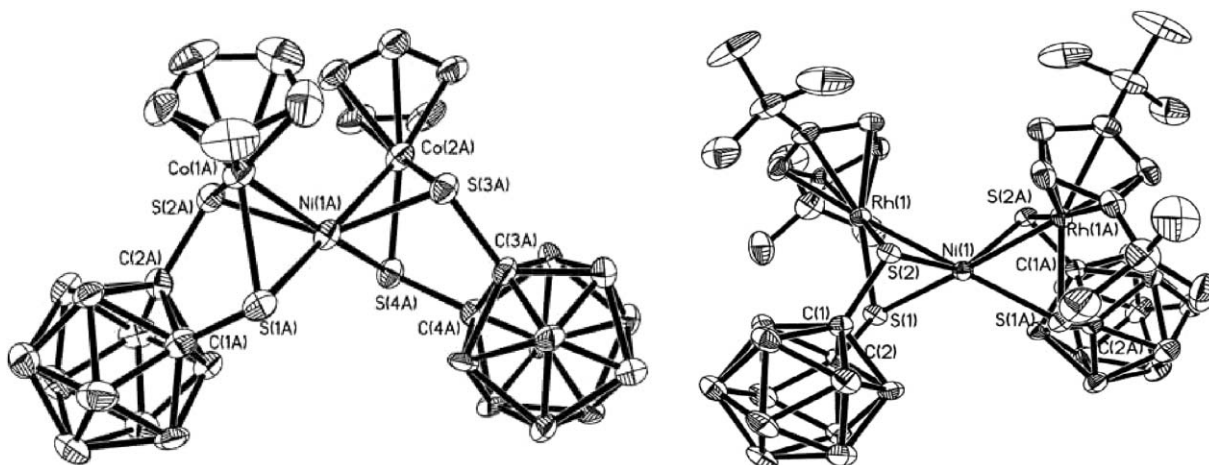
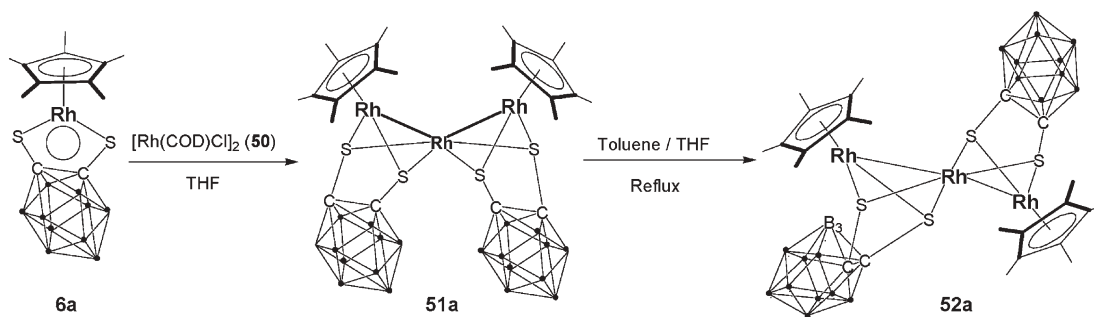


Fig. 13 Molecular structures of 48a and 49a.



Scheme 7 Reaction of **6a** with $[\text{Rh}(\text{COD})(\mu\text{-Cl})_2]$ (**50**).

planes are twisted by 79.1° with respect to one another, and this larger distortion may be attributed to the higher steric hindrance of the Cp' ligand than Cp. The former planar rhodadithiolene heterocycles are curved as a result of the coordination of the S atoms to Ni. The Rh–Ni distances in **49a** (2.458 Å) and **49b** (2.492 Å) may therefore be compared with the corresponding distances in clusters such as $[\text{NiRh}_{14}(\text{CO})_{28}]^{4-}$ (2.481–2.532 Å).³⁷

$[\text{Rh}(\text{COD})(\mu\text{-Cl})_2]$. *cis*- $[\{\text{Cp}^*\text{Rh}[\text{S}_2\text{C}_2(\text{B}_{10}\text{H}_{10})]\}_2\text{Rh}]$ (**51a**) and *trans*- $[\{\text{Cp}^*\text{Rh}[\text{S}_2\text{C}_2(\text{B}_{10}\text{H}_{10})]\}_2\text{Rh}]$ (**52a**) can be prepared from the reaction of **6a** with $[\text{Rh}(\text{COD})(\mu\text{-Cl})_2]$ (**50**), in yields of 25 and 39% respectively (Scheme 7).³⁰ In refluxing THF solution, *cis*-**51a** was converted in more than 95% yield to the *trans*-isomer **52a**. The molecular structures of the two isomers are shown in Fig. 14. In the two complexes, the rhodium atoms of the $[\text{Cp}^*\text{Rh}]$ fragment have been reduced from Rh^{III} to Rh^{II} , apparently by $[\text{Rh}^{\text{I}}(\text{COD})(\mu\text{-Cl})_2]$. The molecule **51a** contains a C_2 axis, and the Rh–Rh length is 2.646 Å. In isomer **52a**, the *o*-carborane groups are drawn sufficiently close to the rhodium center with the distance of $\text{Rh}(1)\cdots\text{B}(3)$ being 3.162 Å. Due to the inducement of the rhodium atom to the neighboring boron atom in the carborane, the Rh–Rh length increases to 2.823 Å in **52a**, and the dihedral angle along the $\text{S}(1)\cdots\text{S}(2)$ vector in the RhS_2C_2 ring decreases to 118.38° compared to 133.98° in **51a**. All these prove the presence of metal-induced B–H activation effects in the formation of isomer **52a**.

The 16-electron complex **7a**, was allowed to react with $[\text{Rh}(\text{COD})(\mu\text{-Cl})_2]$ (**50**) in the molar ratio 2 : 1.³⁰ When the mixture was refluxed in toluene for 48 h, red crystals of binuclear complex $\text{Cp}^*\text{Ir}[\text{S}_2\text{C}_2(\text{B}_{10}\text{H}_9)]\text{Rh}(\text{COD})$ (**53a**) were isolated in 61% yield (Scheme 8), and single crystals can be obtained by slow diffusion of hexane into a concentrated solution of **53a** in toluene at low temperature. The binuclear molecule **53a** contains crystallographically imposed C_s symmetry, with the *o*-carborane-1,2-dithiolate bridging a $[\text{Cp}^*\text{Ir}]$ and a $[\text{Rh}(\text{COD})]$ fragment. The long Ir–Rh separation (3.060 Å) indicates that a weak bonding interaction exists between the two metal atoms. The geometry around the rhodium atom is square-planar, with the metal atom bonded to both sulfido groups and to the two olefinic bonds of an η^4 -cycloocta-1,5-diene ligand. The iridium center adopts a three-legged piano-stool arrangement by coordination with the two sulfur atoms and the boron atom, apart from the η^5 -cyclopentadienyl ligand, if not considering the Ir–Rh bond. The formation of an Ir–B bond is indicated by the appearance of Ir–B resonances in the ^{11}B NMR spectrum at $\delta -19$ ppm,³⁸ and the short Ir–B separation of 2.096 Å.

An investigation of the reactivity of **53a** revealed that the trinuclear complex *trans*- $[\{\text{Cp}^*\text{Ir}[\text{S}_2\text{C}_2(\text{B}_{10}\text{H}_9)]\}\text{Rh}\{\text{S}_2\text{C}_2(\text{B}_{10}\text{H}_{10})\}\text{IrCp}^*]$ (**54a**) can be constructed in approximately 60% yield (Scheme 8), when a mixture of complex **53a** and **7a** in toluene was refluxed.³⁰ A systematic study shows that the **54a** can also be directly obtained through the reaction of **7a** with $[\text{Rh}(\text{COD})(\mu\text{-Cl})_2]$ in the molar ratio of 4 : 1. In the

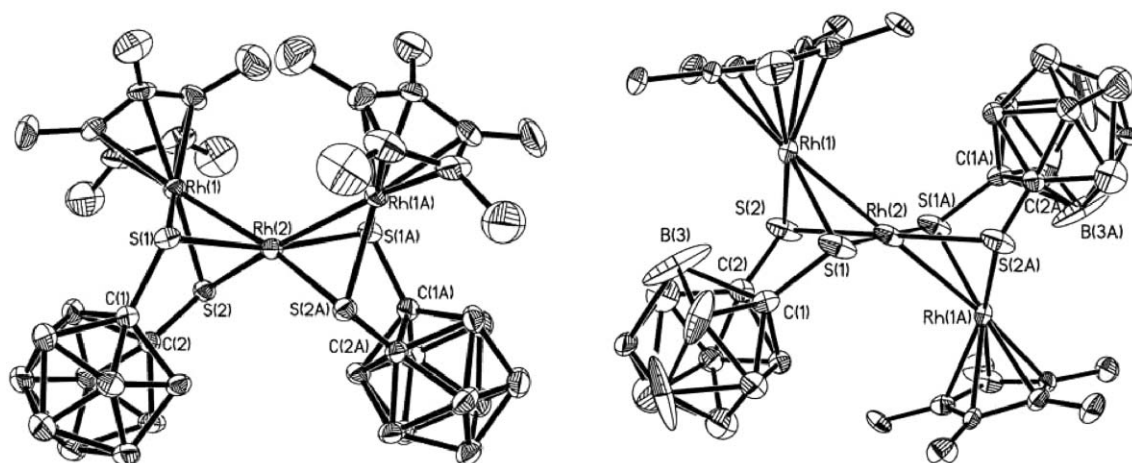
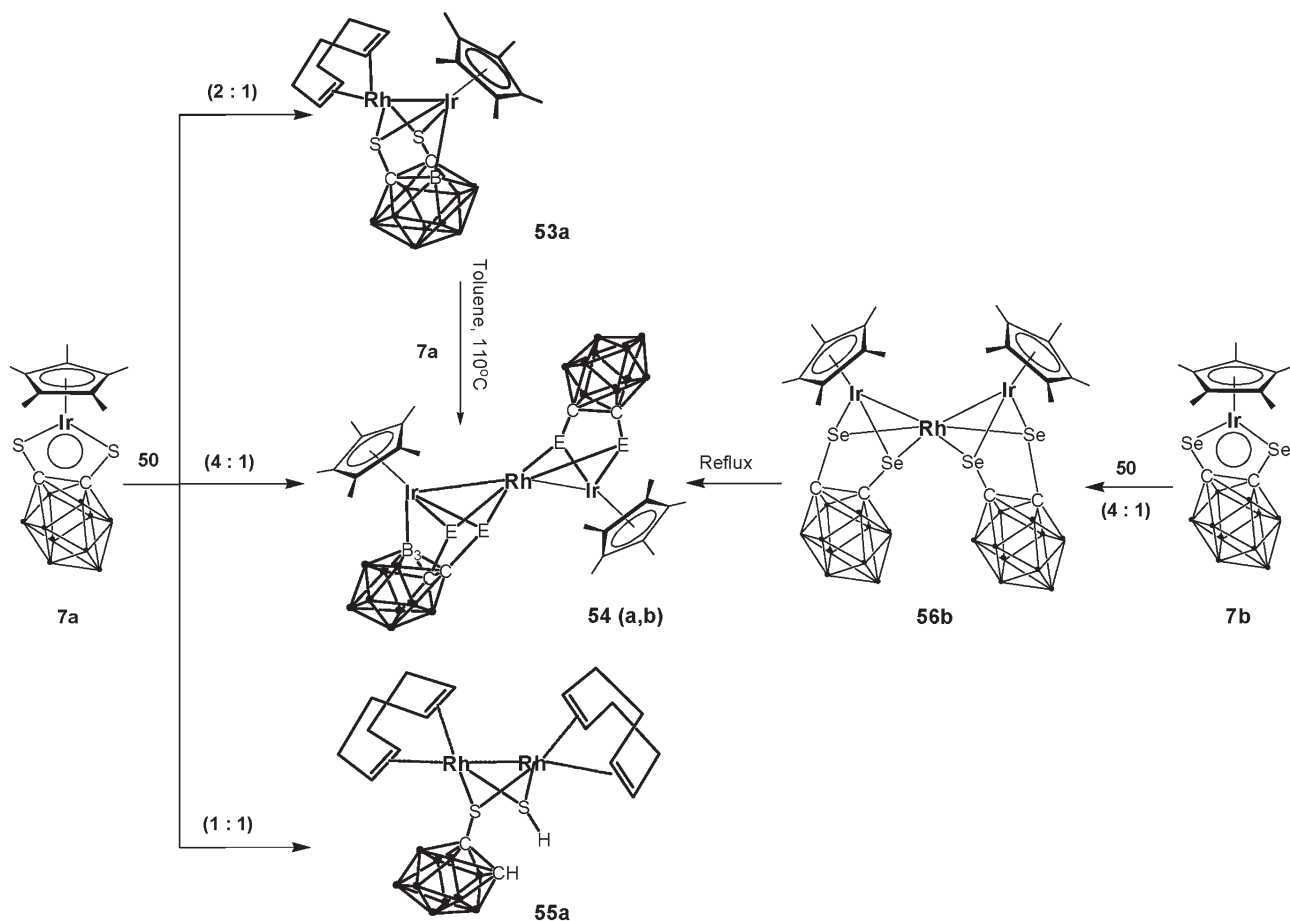


Fig. 14 Molecular structures of **51a** and **52a**.



Scheme 8 Reactions of **7** with $[\text{Rh}(\text{COD})(\mu\text{-Cl})_2]$ (**50**).

complex **54a**, only one of the ancillary *o*-carborane groups contains the Ir–B bond that is present in **53a**. The molecule is therefore asymmetric, as confirmed by the ^1H NMR spectrum with two singlet resonances of the Cp* rings at $\delta = 2.11$ and 2.19 ppm. The X-ray structural analysis also verifies the presence of the Ir–B bond and the two nonequivalent Ir–Rh bonds. The molecular structure shown in Fig. 15 shows a

slightly bent (173.9°) Ir–Rh–Ir backbone. The two iridium atoms have retained their Cp* rings. The Rh center is six-coordinate with distorted octahedral geometry. The Rh atom and the four sulfide ligand atoms are almost coplanar (Rh(1), S(1), S(2), S(3), S(4)). The atom Ir(1) takes a three-legged piano-stool configuration with two four-membered metallacyclic Ir–S–C–B rings. This is due to the cyclometalation of the

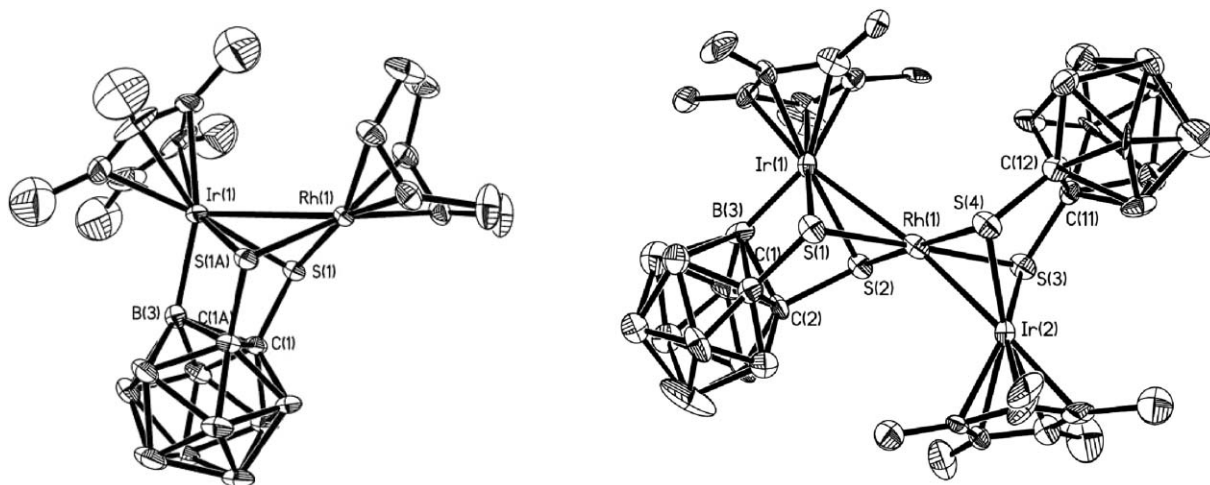


Fig. 15 Molecular structures of **53a** and **54a**.

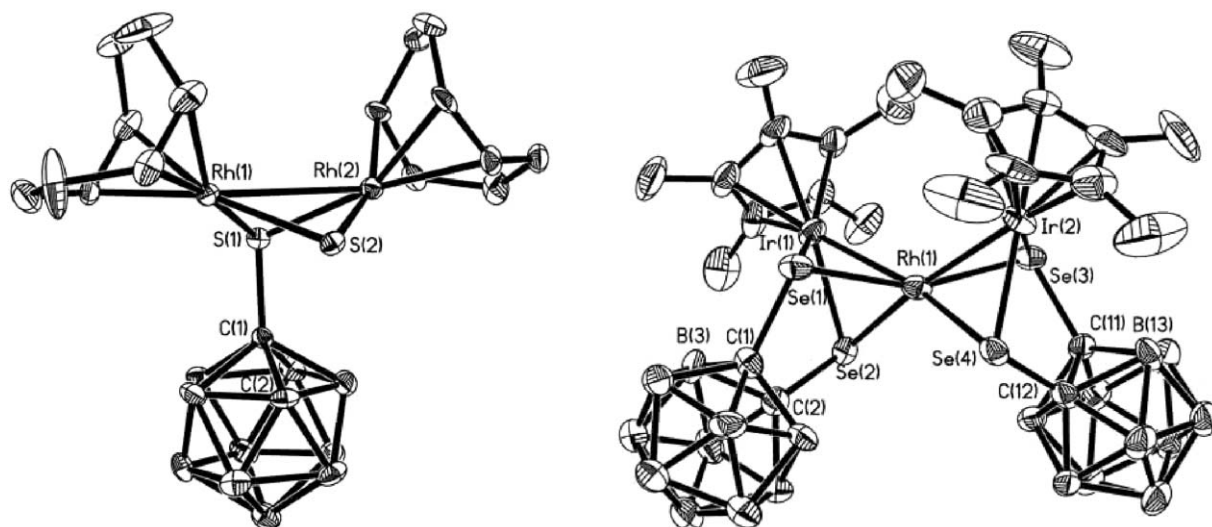


Fig. 16 Molecular structures of **55a** and **56b**.

coordinated dithiolate ligand at the iridium metal center. The Ir(1)–B(3) bond length (2.16 Å) in **54a** is longer than that in **53a**, and the Ir(1)–Rh(1) bond (3.003(3) Å) is longer than the Ir(2)–Rh(1) bond (2.685(3) Å), and this can be rationalized by the fact that the formal oxidation (“valence”) state is +3 for Ir(1) and +2 for Ir(2). Although only a weak interaction can be assumed for the Ir(1)–Rh(1) bond, the Ir(2)–Rh(1) bond length of 2.685(3) Å lies in the expected range for a metal–metal bond.

Refluxing a toluene solution containing a 1 : 1 ratio of Cp*IrS₂C₂(B₁₀H₁₀) (**7a**) and [Rh(COD)(μ-Cl)]₂ can only lead to the formation of homo-bimetallic Rh₂(COD)₂(μ-SH)[(CH)(μ-SC)(B₁₀H₁₀)] (**55a**).³⁰ The ¹H NMR spectrum of **55a** exhibits a carborane (C–H) resonance at δ = 5.31 and an S–H resonance at δ = 0.86 ppm. The X-ray diffraction analysis of the molecular structure for complex **55a** confirms a dinuclear rhodium(I) thiolate complex, which is shown in Fig. 16. The structure differs from that of {(COD)Rh}₂[S₂C₂(B₁₀H₁₀)] (**3a**).¹⁷ Two bridging sulfur atoms and a chelating cyclooctadiene are ligated to each metal atom. The dihedral angle along the Rh(1)⋯Rh(2) vector, between the two planes defined by Rh(1)–Rh(2)–S(1) and Rh(1)–Rh(2)–S(2), is 126.08°. The bond Rh(1)–Rh(2) (3.021 Å) is slightly longer than the intermetallic distances found in the dimer [(Rh(μ-SC₆F₅)(COD))₂] (2.955 Å),³⁹ The S(1)–C(1) separation is 1.790 Å, which can be compared with the C–S separation in {(COD)Rh}₂[S₂C₂(B₁₀H₁₀)] (**3a**).¹⁷ On the other hand, the S(2)–C(2) bond is cleaved and the distance is 3.354 Å. The Rh–S bond lengths, 2.359–2.425 Å, are statistically slightly different.

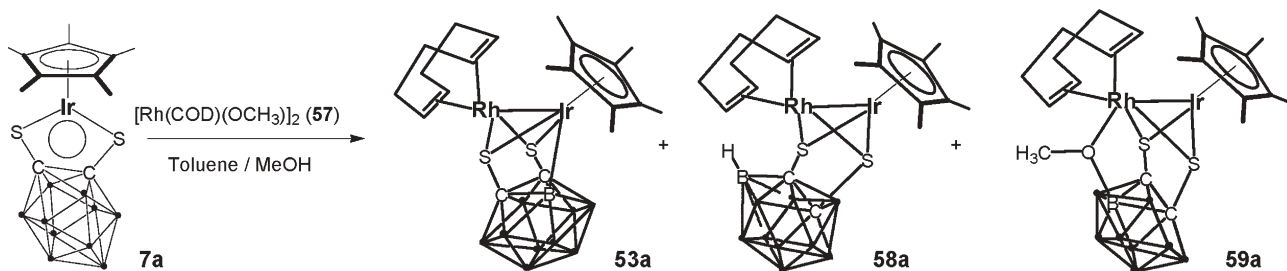
On reaction of **7b** with [Rh(COD)(μ-Cl)]₂ in THF for three days, the cisoid **56b** and transoid **54b** can be isolated in 38 and 32% yield, respectively.²⁶ In refluxing toluene solution, complex **56b** can be converted in more than 90% yield to **54b** (Scheme 8), which contains a boron–iridium bond. The structure of complex **56b** is similar with that of **54b** in that the four selenium atoms of the two *ortho*-carborane diselenolato ligands surround the central rhodium atom in a distorted tetrahedral arrangement. The Ir–Rh distances are 2.7097 and 2.6630 Å. The two Se–Rh–Se planes are twisted by 63.1° with

respect to each other. In **54b**, as in **54a**, the iridium atoms of the Ir₂Rh backbone have retained their Cp* rings in a transoid arrangement. One of the two *ortho*-carborane groups is drawn sufficiently close to the iridium center to initiate B–H activation, affording the corresponding cyclometalated species. Similar with **54a**, one of the Ir–Rh bonds (3.074 Å) in **54b** is longer than the other (2.663 Å).

[Rh(COD)(μ-OMe)]₂ and [Ir(COD)(μ-OMe)]₂. Following the observation of B–H activation during the process of building homo- or hetero-multimetallic complexes as discussed previously, studies have been expanded to rational synthesis of the cup-shaped *nido*-carborane complexes, starting from iridium complexes Cp*Ir[E₂C₂(B₁₀H₁₀)] (**7**). It appears to provide useful structural information for further studies on the preparation of other *nido*-carborane and polymetallic species.

Reaction of 2 equiv. of Cp*Ir[S₂C₂(B₁₀H₁₀)] (**7a**) with [Rh(COD)(μ-OMe)]₂ (**57**) in a refluxing toluene–methanol mixture yields the dimetallic Cp*Ir[S₂C₂(B₁₀H₁₀)]Rh(COD) (**58a**, 10%) and formerly studied Cp*Ir[S₂C₂(B₁₀H₉)]Rh(COD) (**53a**, 32%),³⁰ two products that would be expected to arise from different B–H activation processes at the B(3)/B(6) sites of the carborane cage (Scheme 9).⁴⁰ There is a competition between the activities of the two metallic sites: if the iridium atom approaches the B–H site the result is the formation of **53a**, whereas the approach of the rhodium atom to the B–H site leads to **58a**. It may be noted that the cyclometalation occurs at the iridium, not at the rhodium site. More importantly, IrRh-*nido*-carborane Cp*Ir[S₂C₂(B₉H₉)][(COD)Rh(OCH₃)] (**59a**) can be isolated as the third band *via* chromatography in 41% yield. All these differences can be partially ascribed to the formally different valence state of iridium and rhodium atoms before the reaction, and iridium is also a stronger inducing agent of B–H activation than rhodium.

In **58a**, the *o*-carborane group is close to the rhodium center (Rh(1)⋯B(3) 2.970 Å). An interesting phenomenon is that the B(3) atom appears to have the tendency to leave the cage. This can also be confirmed by the lengthening of the C(1)–B(3) and



Scheme 9 Reaction of **7a** with $[\text{Rh}(\text{COD})(\mu\text{-OMe})]_2$ (**57**).

C(2)–B(3) bonds (1.78(4) and 1.84(4) Å, respectively), in contrast to 1.72 Å under normal conditions.⁴¹ The Ir–Rh distance in **58a** (2.7829(10) Å) is much shorter than that in **53a** (3.060 Å), due to the difference in oxidation states of the metal centers.

The NMR spectra and crystal structure determination show that the cluster framework adopted by **59a** is generated by incorporation of a *nido*-C₂B₉ unit into a Rh–Ir metal complex (Fig. 17). In **59a**, the [Cp*Ir] and [(COD)Rh] fragments are bridged by two S atoms that links to the open C₂B₃ face. The metal atoms are arranged at one side of the cup-shaped *nido*-carborane just like the handle of a cup. The Ir–Rh distances of

2.7526 Å fall within the expected range of metal–metal single bonds; consequently each metal center has 18 valence electrons and thus accounts for the diamagnetism observed for these complexes.

Similar reactions with iridium complexes were investigated (Scheme 10).⁴⁰ After treatment of Cp*Ir[E₂C₂(B₁₀H₁₀)] (**7**) with $[\text{Ir}(\text{COD})(\mu\text{-OMe})]_2$ (**60**), an analogous dimetallic Ir–Ir–*nido*-carborane product Cp*Ir[E₂C₂(B₉H₉)]{(COD)Ir(OCH₃)} (**61**) was obtained (Fig. 18). Based on spectrometry and crystallographic characterization, complexes **61** (a, b) share a similar framework with the hetero-metallic complex **59a**. The Ir(1)–Ir(2) distances of 2.7250 Å (**61a**) and 2.8087 Å (**61b**) fall

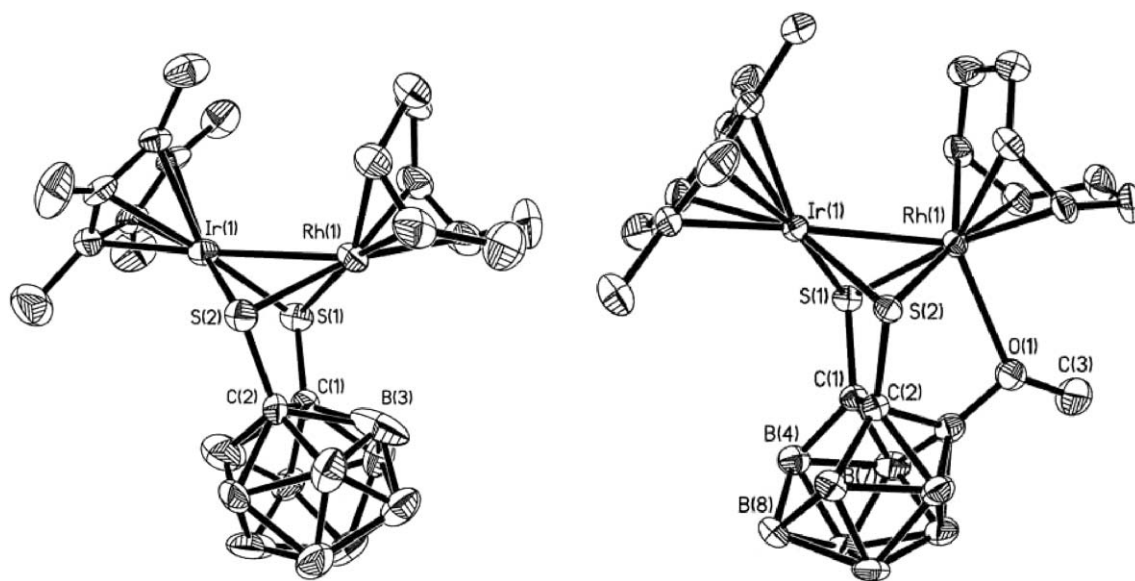
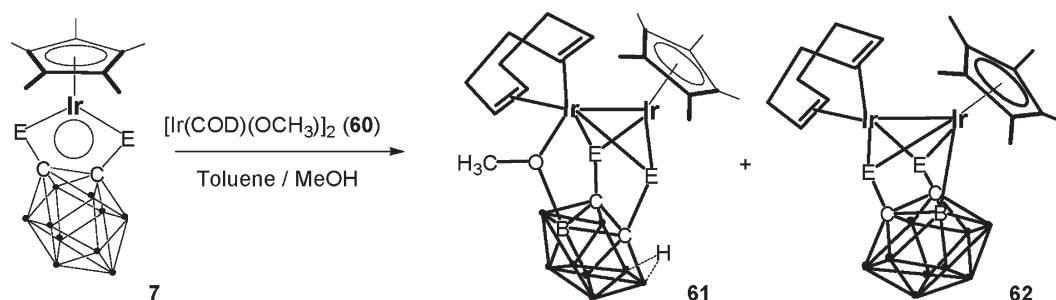


Fig. 17 Molecular structures of **58a** and **59a**.



Scheme 10 Reaction of **7** with $[\text{Ir}(\text{COD})(\mu\text{-OMe})]_2$ (**60**).

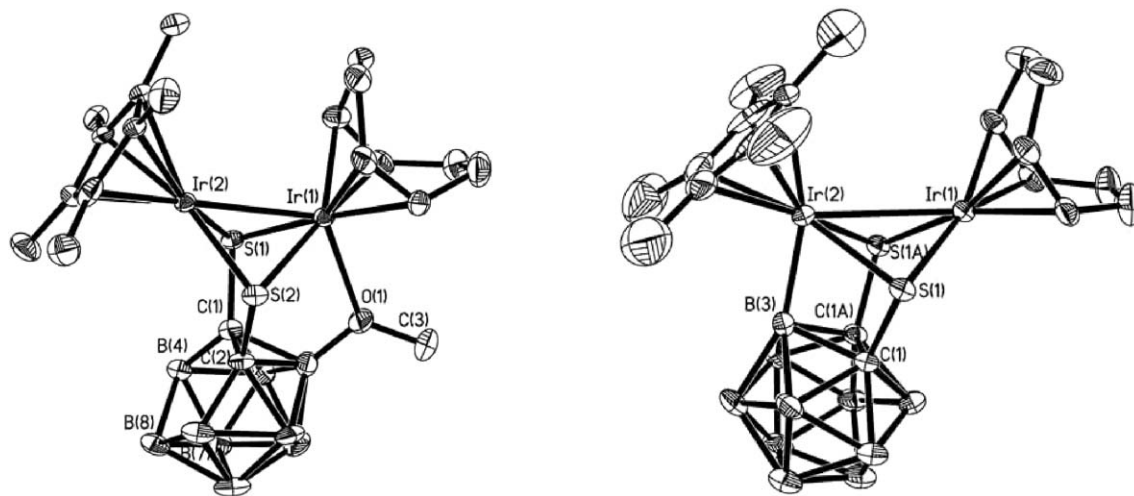


Fig. 18 Molecular structures of **61a** and **62a**.

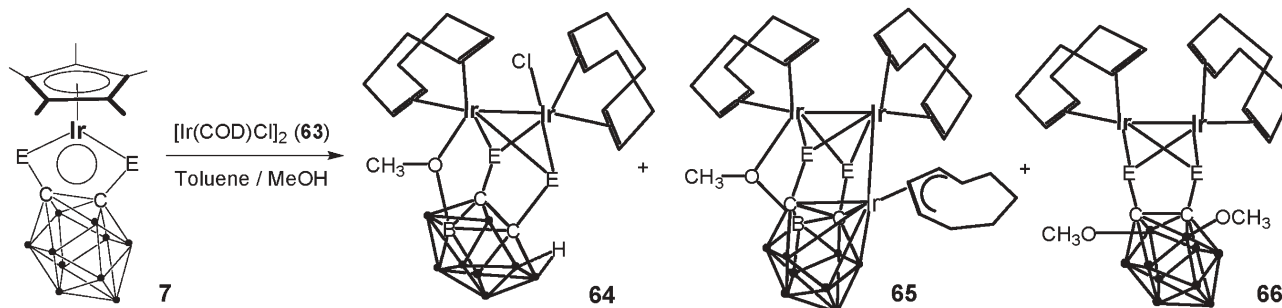
within the expected range of metal–metal single bonds. $\text{Cp}^*\text{Ir}[\text{S}_2\text{C}_2(\text{B}_{10}\text{H}_9)]\text{Ir}(\text{COD})$ (**62**) can be isolated as the minor product, and is characterized by X-ray structure analysis. The presence of an Ir–B bond indicates the activation of B–H, which is clearly induced by the metal atom. Complexes **61** can be obtained in higher yields when longer reaction times are applied. Hence it can be assumed that **62** are the intermediates with reactive Ir–B bonds. Generated after the iridium-induced B–H activation, they then undergo cage-opening process to give the concomitant formation of **61**.

$[\text{Ir}(\text{COD})(\mu\text{-Cl})_2]$. Heating **7** with 4 equiv. of $[\text{Ir}(\text{COD})(\mu\text{-Cl})_2]$ (**63**) in the presence of MeOH generates *nido*- $\{(\text{COD})\text{Ir}(\text{OCH}_3)\}[\text{E}_2\text{C}_2(\text{B}_9\text{H}_9)]\{(\text{COD})\text{IrCl}\}$ (**64**) as the major product, as well as the minor products $\{(\text{COD})\text{Ir}\}_2[\text{E}_2\text{C}_2(\text{B}_9\text{H}_8)(\text{OCH}_3)\{\text{Ir}(\eta^3\text{-COD})\}]$ (**65**) and $\{(\text{COD})\text{Ir}\}_2[\text{E}_2\text{C}_2(\text{B}_{10}\text{H}_8)(\text{OCH}_3)_2]$ (**66**) (Scheme 11).⁴⁰ In refluxing toluene–methanol solution, the bimetallic clusters **64** are converted in more than 60% yield to the trimetallic complexes **65** when additional $[\text{Ir}(\text{COD})(\mu\text{-Cl})_2]$ (**63**) is applied.

An X-ray diffraction study of **64a** provided additional interesting features for this kind of *nido*-carborane complex (Fig. 19). Both iridium centers are in a distorted octahedral environment. The difference between the two iridium atoms is that the Ir(2) center bears a bridging OCH_3 ligand, whereas the

Ir(1) center carries a terminal chloride ligand, in addition to the olefinic bonds of the COD ligands and the bridging sulfur atoms. Considering that the 14-electron fragments $[\text{Cp}^*\text{Ir}]$ and $\{(\text{COD})\text{IrCl}\}$ are isolobal, other crystallographic parameters are comparable with **62**, for example the Ir–Ir bond lengths (2.7250 Å in **61a** and 2.7379(8) Å in **64a**).

What more exciting is the isolation of **65**, the products with three metal atoms in a cluster, as confirmed by X-ray diffraction for **65b** (Fig. 19). The Ir(3) atom is coordinated to the C_2B_3 pentagonal open face and to the three allylic carbon atoms of a cyclooctenyl ligand. The Ir(2)–Ir(3) distance (3.0866 Å) is lengthened compared with Ir(1)–Ir(2) (2.9473(10) Å). Interestingly, the C(1)–C(2) distance (1.81 Å) is longer than a normal bond between the two carbon atoms of a carborane, but shorter than those in the pseudo-*closo*-metallacarborane structure.⁴² The lengthening of the C(1)–C(2) distance in **65b** produced a tetragonal open face Ir(3)–C(1)–C(2)–B(6), which is almost planar, with a dihedral angle along C(1)–C(2) of 163.7°. Complexes of type **65** represent a novel class of cluster compounds in which a V-shaped trimetallic unit has been constructed through a new type of M-*nido*-carborane complex. It is also the first structural confirmation of a trinuclear metallic cluster that represents an unprecedented example of a metallacarborane complex featuring intercluster metal–metal bonds.



Scheme 11 Reaction of **7** with $[\text{Ir}(\text{COD})(\mu\text{-Cl})_2]$ (**63**).

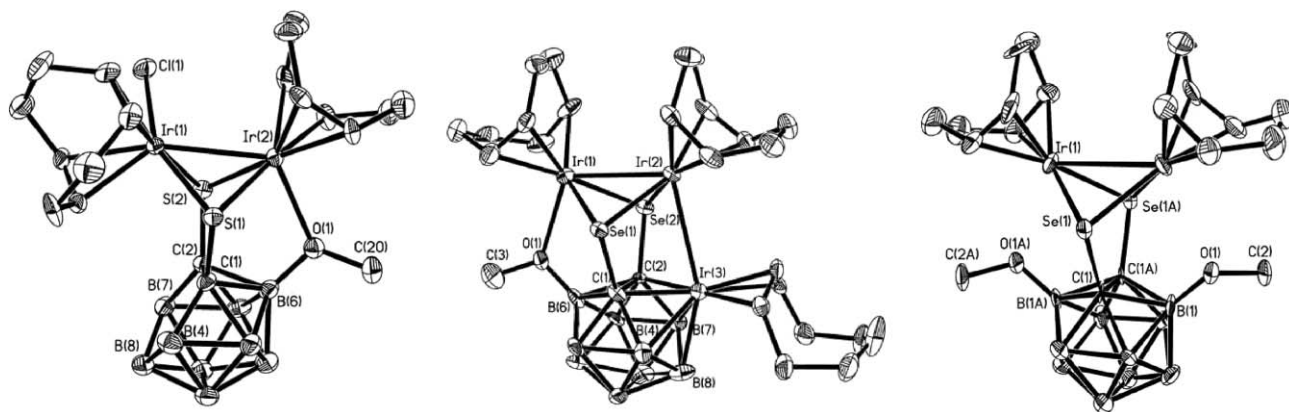


Fig. 19 Molecular structures of **64a**, **65b** and **66b**.

In the byproduct complexes **66** of the reaction, both the B(3)/B(6) sites of the carborane ligand are substituted with methoxy groups and the Ir–Ir distance is 2.8939 Å (Fig. 19).

[Rh(COD)(μ-OEt)]₂. As discussed previously, the dimer **[Rh(COD)(μ-Cl)]₂** (**50**) was an acceptable material to produce Ir₂Rh trinuclear metallic clusters such as **54**. Taking into account that **[Rh(COD)(μ-OEt)]₂** (**67**) has been long known to be a useful precursor to prepare a variety of rhodium complexes, the similar reaction with **7** was carried out.

Complex **7** reacted with **[Rh(COD)(μ-OEt)]₂** (**67**) in the molar ratio 2 : 1 in toluene, and two products, namely *trans*-[Cp*Ir[E₂C₂(B₁₀H₉)]Rh{[E₂C₂(B₁₀H₁₀)]IrCp*}] (**54**) and (COD)Rh{Cp*Ir[E₂C₂(B₁₀H₉)]Rh{Cp*Ir[E₂C₂(B₁₀H₁₀)]} (**68**) were obtained in moderate yield (Scheme 12).⁴³ Complexes **68** can be obtained in higher yields when longer reaction times are applied.

Compared with the structures of **54**, the difference lies in the [(COD)Rh] fragment in **68**. It can be presumed that in the whole reaction the [(COD)Rh] fragment exists in some reactive form and inserts into the original S(3)–C(3) bond, accompanying the cleavage of S(3)–C(3) bond, and **68** is formed, though further investigations of these aspects are in progress.

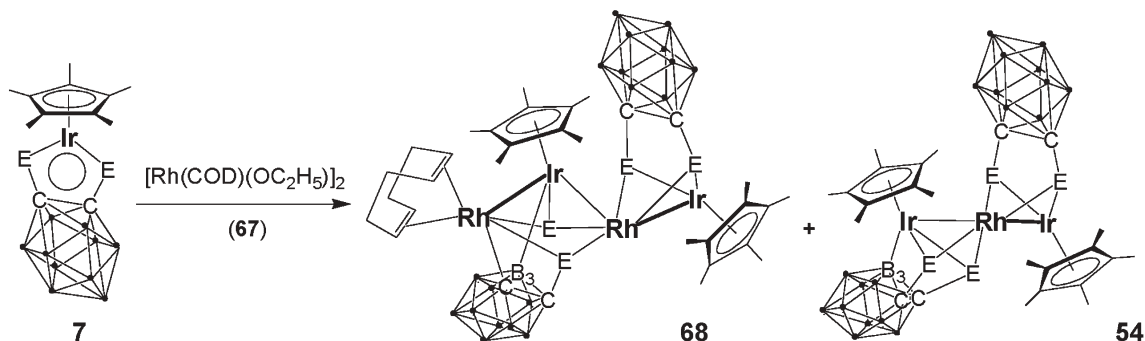
The molecular structure of **68a** is shown in Fig. 20. The metal atoms of the core adopt a nearly planar Ir₂Rh₂ arrangement, which is rare to our knowledge.⁴⁴ The two dithiolato ligands of carboranes are situated at the both sides of the *tetra*-metallic plane with three sulfur atoms acting

as μ₂-bridging ligands and one sulfide simultaneously connecting three metals. If COD is considered as a bidentate ligand, Rh(1) and Rh(2) metals both exhibit six-coordinate environments, and Ir(1) shows a similar coordination sphere of that in **54a** with a three-legged piano-stool configuration. In contrast, Ir(2) coordinates to a clearly different set of ligands, boron and two metal bonds with Rh(1) and Rh(2), except for the similar Cp* and bridging thiolate ligands. By using the thiolate ligands, Rh(2) connects the Ir(1) and Ir(2) atoms, and the bond lengths are 2.5990 Å (Rh(2)–Ir(1)) and 2.9814 Å (Rh(2)–Ir(2)), respectively. Compared with the analogous fragment in **54a** (2.685 Å), the Rh(2)–Ir(1) metal bond becomes much shorter. The presence of a shorter d⁸–d⁸ Ir(1)–Rh(2) interaction in **68a** is also supported by the Ir(1)–S–Rh(2) angles (66.76 and 66.48°), which are smaller than the analogous Rh–S–Ir angles in **54a** (69.59 and 69.8°). The third metal–metal bond formed by Ir(2)–Rh(1) (2.7862 Å), falls in the expected range for a single bond.

3.3 Half-sandwich reagents with Cp ligand

CpCo(CO)₂ and **CpCo(C₂H₄)₂**. Although plenty of organo-metallic clusters with dithiolene ligands have been synthesized and characterized, the dinuclear complexes, in which both the metal centers adopt half-sandwich configurations, have not been fully investigated.

The first attempt to prepare hetero-bimetallic Rh–Co complexes (Cp*Rh)[E₂C₂(B₁₀H₁₀)](CpCo) (**71**) involved the



Scheme 12 Reaction of **7** with **[Rh(COD)(μ-OEt)]₂** (**67**).

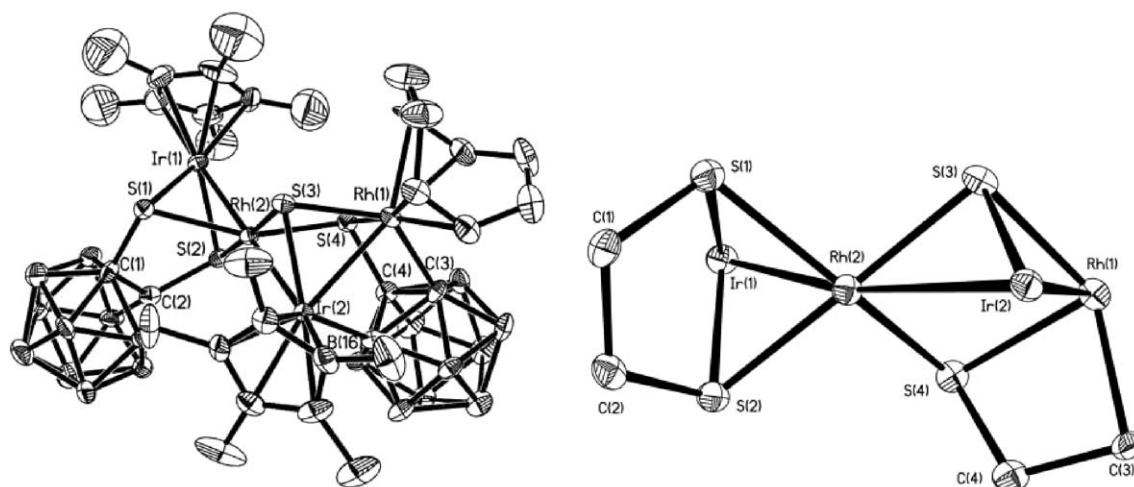
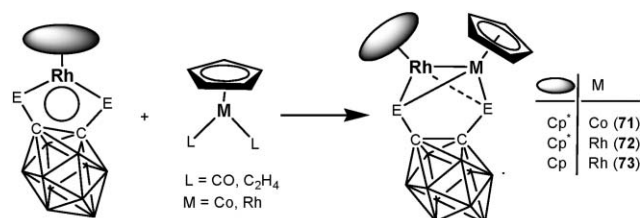


Fig. 20 Molecular structure and backbone of **68a**.

treatment of 16-electron precursors **6** with an equivalent of $\text{CpCo}(\text{C}_2\text{H}_4)_2$ (**69**) (Scheme 13).¹⁹ Additionally, **71** could also be generated through the reaction of **6** with $\text{CpCo}(\text{CO})_2$ (**70**) in the presence of Me_3NO , and the yields could be increased by nearly 10% upon heating.⁴⁵ The molecular structure of **71a**, established by X-ray analysis at room temperature (Fig. 21), suggests that there is a mirror plane going through the Rh–Co backbone. The metal centers are connected to both sulfido atoms and to the Cp* (or Cp) rings, adopting a three-legged piano-stool arrangement. The Rh(1)–Co(1) distance (2.4777 Å)

indicates strong bonding interaction between the two metal atoms, and is short if compared with those in the trinuclear complex $\text{Cp}^*\text{Rh}[\text{E}_2\text{C}_2(\text{B}_{10}\text{H}_{10})][\text{Co}_2(\text{CO})_5]$ (**43a**; 2.6057, 2.6399 Å).²⁹ The rhodadithiolate hetero-cycle (Rh(1)–S(1)–C(1)–C(1A)–S(1A)) in **71a** is bent with a dihedral angle along the S(1)⋯S(1A) vector of 131.6°, due to the addition of the [CpCo] moiety. The selenium counterpart **71b** possesses a similar structure as **71a** and the Rh–Co bond (2.5101 Å) is comparable to **71a**.



Scheme 13 Reactions with $\text{CpCo}(\text{C}_2\text{H}_4)_2$ (**69**), $\text{CpCo}(\text{CO})_2$ (**70**) and $\text{CpRh}(\text{C}_2\text{H}_4)_2$ (**74**).

$\text{CpRh}(\text{C}_2\text{H}_4)_2$. This facile synthetic approach was also successful for the analogous dinuclear Rh–Rh complexes, namely $(\text{Cp}^*\text{Rh})[\text{E}_2\text{C}_2(\text{B}_{10}\text{H}_{10})](\text{CpRh})$ (**72**) and $(\text{CpRh})_2[\text{S}_2\text{C}_2(\text{B}_{10}\text{H}_{10})]$ (**73a**), through treatment of **6** or **11a** with $\text{CpRh}(\text{C}_2\text{H}_4)_2$ (**74**), taking advantage of ethylene as a good leaving group.⁴⁵ In all these three complexes, the rhodium fragments of the original carborane precursors have been reduced from Rh^{III} to Rh^{II} , apparently by **74**. Molecular structures have been determined by X-ray analysis using single crystals grown from hexane solutions. The Rh–Rh bond lengths are 2.5722 (**72a**), 2.6106 (**72b**) and 2.5627 (**73a**) Å,

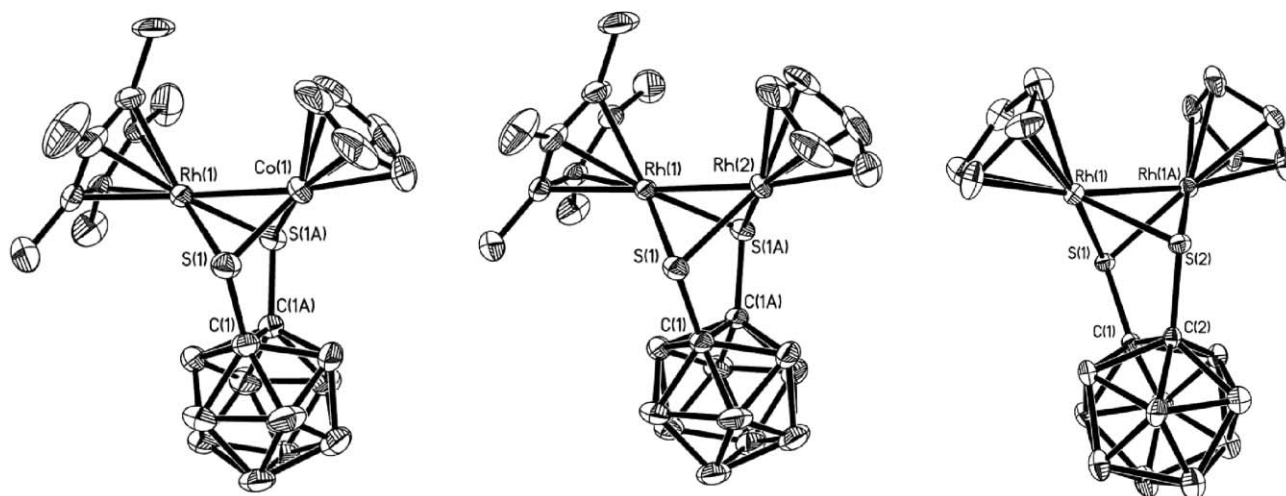
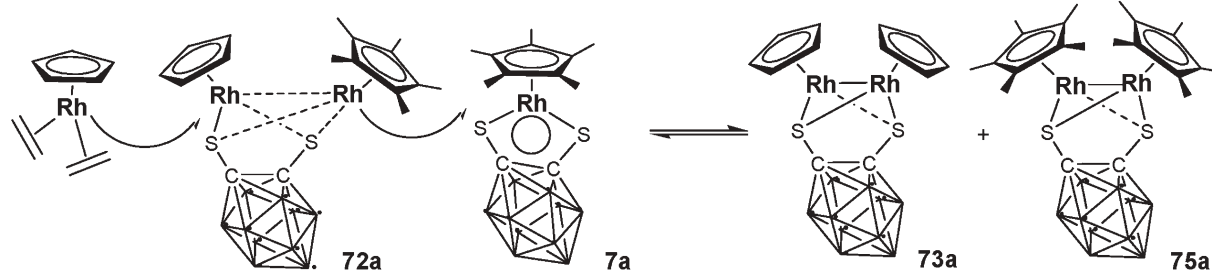


Fig. 21 Molecular structures of **71a**, **72a** and **73a**.



Scheme 14 Proposed reaction route to give 73a and 75a.

which are comparable with those in the previously reported complexes $(\text{Cp}^*\text{Rh})_2[\text{S}_2\text{C}_2(\text{B}_{10}\text{H}_{10})]$ (75a; 2.6245 Å)²⁹ and $(\text{Cp}'\text{Rh})_2[\text{E}_2\text{C}_2(\text{B}_{10}\text{H}_{10})]$ (76a; 2.5654 Å)²⁵ and also correspond to metal–metal single bonds. Interestingly, complexes 73a and 75a can also be isolated as by-products in very low yields from the preparation of 72a, if a slight excess of $\text{CpRh}(\text{C}_2\text{H}_4)_2$ is present and longer reaction times are employed (Scheme 14).

4 Summary and perspectives

Considerable progress has been made on metal–metal bond formation *via* 1,2-dicarba-closo-dodecarborane-1,2-dichalcogenolates during the past decade, which makes it an indispensable approach of rational design for homo- and hetero-multimetallic clusters. This review article summarizes briefly the methodology of taking advantage of the redox reactions between the pseudo-aromatic carborane-1,2-dichalcogenolato cobalt(III), rhodium(III), iridium(III) or ruthenium(II) complexes and low-valent organometallic reagents. Combined analytical tools of X-ray crystallography and spectroscopic characterizations are introduced to confirm the formation of direct metal–metal bonds and study the nature of the reaction route. In addition, metal-induced B–H activation can be accomplished by tailoring the reaction precursors and the reaction conditions, which provides systematic information for further studies on the preparation of cup-shaped *nido*-carborane complexes or metallacarborane complexes.

Given the relatively mild reaction conditions, moderate yields, as well as the ease of characterization and crystallization of the target products, it can be anticipated that the pseudo-aromatic carborane–dichalcogenolate compounds are promising precursors for the investigation of the chemistry of various homo- and hetero-multimetallic clusters. More importantly, the extensive study of this pseudo-aromatic carborane system also ignites the exploration of organometallic cluster-based assemblies^{46,47} and the potential applications of multimetallic entities as well.

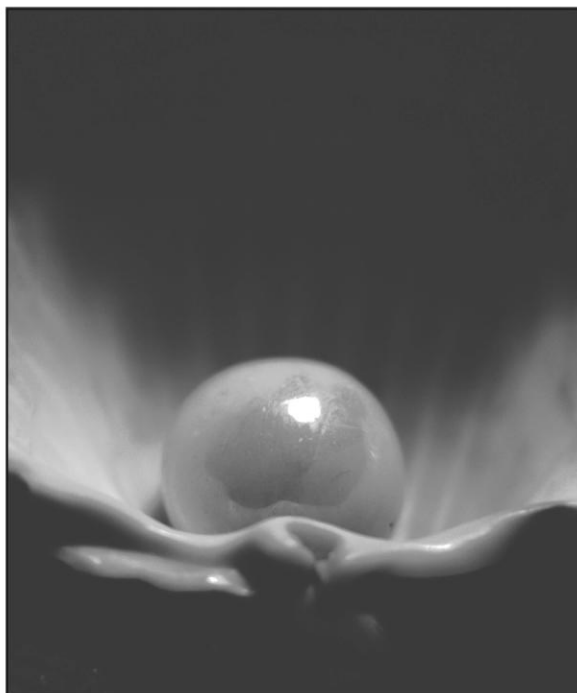
Acknowledgements

We are grateful to financial support by the National Science Foundation of China for Distinguished Young Scholars (20421303, 20531020), by the National Basic Research Program of China (2005CB623800) and by Shanghai Science and Technology Committee (05JC14003, 05DZ22313).

References

- 1 L. H. Gade, *Angew. Chem., Int. Ed.*, 2000, **39**, 2658.
- 2 M. C. Comstock and J. R. Shapley, *Coord. Chem. Rev.*, 1995, **143**, 501.
- 3 B. Bosnich, *Inorg. Chem.*, 1999, **38**, 2554.
- 4 E. K. van den Beuken and B. L. Feringa, *Tetrahedron*, 1998, **54**, 12985.
- 5 H. T. Chifotides and K. R. Dunbar, *Acc. Chem. Res.*, 2005, **38**, 146.
- 6 H. Wadepohl, A. Metz and H. Pritzkow, *Chem.–Eur. J.*, 2002, **8**, 1591.
- 7 V. N. Kokozay and O. Y. Vassilyeva, *Transition Met. Chem.*, 2002, **27**, 693.
- 8 R. E. P. Winpenny, *J. Chem. Soc., Dalton Trans.*, 2002, 1.
- 9 K. Severin, *Chem.–Eur. J.*, 2002, **8**, 1514.
- 10 R. Y. C. Shin and L. Y. Goh, *Acc. Chem. Res.*, 2006, **39**, 301.
- 11 E. Sappa, A. Tiripicchio and P. Braunstein, *Chem. Rev.*, 1983, **83**, 203.
- 12 M. Nihei, T. Nankawa, M. Kurihara and H. Nishihara, *Angew. Chem., Int. Ed.*, 1999, **38**, 1098.
- 13 M. Fourmigue, *Coord. Chem. Rev.*, 1998, **178–180**, 823.
- 14 R. B. King, *Chem. Rev.*, 2001, **101**, 1119.
- 15 G.-X. Jin, *Coord. Chem. Rev.*, 2004, **248**, 587.
- 16 S. X. Lu, G.-X. Jin, S. Eibl, M. Herberhold and Y. Xin, *Organometallics*, 2002, **21**, 2533.
- 17 S. Y. Cai, X. F. Hou, L. H. Weng and G.-X. Jin, *J. Organomet. Chem.*, 2005, **690**, 910.
- 18 M. Herberhold, H. Yan and W. Milius, *J. Organomet. Chem.*, 2000, **598**, 142.
- 19 D. H. Kim, J. J. Ko, K. Park, S. G. Cho and S. O. Kang, *Organometallics*, 1999, **18**, 2738.
- 20 M. Herberhold, G.-X. Jin, H. Yan, W. Milius and B. Wrackmeyer, *J. Organomet. Chem.*, 1999, **587**, 252.
- 21 J. Y. Bae, Y. I. Park, J. J. Ko, K. I. Park, S. I. Cho and S. O. Kang, *Inorg. Chim. Acta*, 1999, **289**, 141.
- 22 A. N. Nesmeyanov, V. V. Krivykh, V. S. Kaganovich and M. I. Rybinskaya, *J. Organomet. Chem.*, 1975, **102**, 185.
- 23 Y. Q. Chen, J. Zhang, S. Y. Cai, X. F. Hou, H. Schumann and G.-X. Jin, *Dalton Trans.*, 2007, 749.
- 24 S. Y. Cai, Y. J. Lin and G.-X. Jin, *Dalton Trans.*, 2006, 912.
- 25 S. Y. Cai, J. Q. Wang and G.-X. Jin, *Organometallics*, 2005, **24**, 4226.
- 26 G.-X. Jin, J. Q. Wang, C. Zhang, L. H. Weng and M. Herberhold, *Angew. Chem., Int. Ed.*, 2005, **44**, 259.
- 27 S. Liu, X. Wang and G.-X. Jin, *J. Organomet. Chem.*, 2006, **691**, 261.
- 28 W. Li, L. H. Weng and G.-X. Jin, *Inorg. Chem. Commun.*, 2004, **7**, 1174.
- 29 S. Y. Cai and G.-X. Jin, *Organometallics*, 2005, **24**, 5280.
- 30 J. Q. Wang, S. Y. Cai, G.-X. Jin, L. H. Weng and M. Herberhold, *Chem.–Eur. J.*, 2005, **11**, 7342.
- 31 J. Q. Wang, L. H. Weng and G.-X. Jin, *J. Organomet. Chem.*, 2005, **690**, 249.
- 32 S. Y. Cai, X. F. Hou, Y. Q. Chen and G.-X. Jin, *Dalton Trans.*, 2006, 3736.
- 33 J. Q. Wang, X. F. Hou, L. H. Weng and G.-X. Jin, *Organometallics*, 2005, **24**, 826.

- 34 F. A. Cotton and J. M. Troup, *J. Am. Chem. Soc.*, 1974, **96**, 4155.
- 35 X. Y. Yu, S. X. Lu, G.-X. Jin and L. H. Weng, *Inorg. Chim. Acta*, 2004, **357**, 361.
- 36 L. R. Byers, V. A. Uchtman and L. F. Dahl, *J. Am. Chem. Soc.*, 1981, **103**, 1942.
- 37 C. Femoni, F. Demartin, M. C. Iapalucci, A. Lombardi, G. Longoni, C. Marin and P. H. Svensson, *J. Organomet. Chem.*, 2000, **614**, 294.
- 38 E. L. Hoel and M. F. Hawthorne, *J. Am. Chem. Soc.*, 1974, **96**, 6770.
- 39 D. Cruz-Garriz, B. Rodriguez, H. Torrens and J. Leal, *Transition Met. Chem.*, 1984, **9**, 284.
- 40 J. Q. Wang, M. Herberhold and G.-X. Jin, *Organometallics*, 2006, **25**, 3508.
- 41 J. M. Oliva, N. L. Allan, P. V. Schleyer, C. Vinas and F. Teixidor, *J. Am. Chem. Soc.*, 2005, **127**, 13538.
- 42 I. T. Chizhevsky, I. A. Lobanova, P. V. Petrovskii, V. I. Bregadze, F. M. Dolgushin, A. I. Yanovsky, Y. T. Struchkov, A. L. Chistyakov, I. V. Stankevich, C. B. Knobler and M. F. Hawthorne, *Organometallics*, 1999, **18**, 726.
- 43 G.-X. Jin and J. Q. Wang, *Dalton Trans.*, 2006, 86.
- 44 J. R. Galsworthy, A. D. Hattersley, C. E. Housecroft, A. L. Rheingold and A. Waller, *J. Chem. Soc., Dalton Trans.*, 1995, 549.
- 45 S. Liu and G.-X. Jin, *Dalton Trans.*, 2007, 949.
- 46 J. Q. Wang, C. X. Ren, L. H. Weng and G.-X. Jin, *Chem. Commun.*, 2006, 162.
- 47 S. Liu, J. S. Zhang, X. Wang and G.-X. Jin, *Dalton Trans.*, 2006, 5225.



Looking for that **special**
research paper from applied
and technological aspects of the
chemical sciences?

TRY this free news service:

Chemical Technology

- highlights of newsworthy and significant advances in chemical technology from across RSC journals
- free online access
- updated daily
- free access to the original research paper from every online article
- also available as a free print supplement in selected RSC journals.*

*A separately issued print subscription is also available.

Registered Charity Number: 207890

22030683

RSC Publishing

www.rsc.org/chemicaltechnology